Aus der Klinik für Psychiatrie und Psychotherapie

Geschäftsführender Direktor Univ.-Prof. Dr. med. T. Kircher

des Fachbereichs Medizin der Philipps-Universität Marburg

in Zusammenarbeit mit dem Universitätsklinikum Gießen und Marburg GmbH

Standort Marburg

Exploration of material dependent memory lateralization of the hippocampus and adjourning anatomical regions by fMRI

Inaugural-Dissertation zur Erlangung des Doktorgrades der gesamten Humanmedizin

dem Fachbereich Medizin der Philipps-Universität Marburg

vorgelegt von:

David Johannes Brandt aus Münster

Marburg, 2013

Angenommen vom Fachbereich Medizin der Philipps-Universität Marburg
am: 30.10.2013

Gedruckt mit Genehmigung des Fachbereichs.

Dekan: Univ.-Prof. Dr. H. Schäfer

Referent: Univ.-Prof. Dr. A. Jansen

Korreferent: Univ.-Prof. Dr. S. Knake

Für meine Eltern

Table of contents

Table of Figures

Table of Tables

List of Abbreviations

BOLD:	Blood oxygen level dependent
EEG:	Elektroencephalography
fMRI:	Functional magnetic resonance imaging
fTCD:	Functional transcranial Doppler sonography
GM:	Grey matter
ICC:	Intraclass correlations
LI:	Lateralization index
MEG:	Magnetoencephalography
MRI:	Magnetic resonance imaging
MTL:	Medial temporal lobe
ROI:	Region of interest

Zusammenfassung

Das Prinzip der funktionellen Asymmetrie, also die Aufteilung der Hirnfunktionen zwischen den Hirnhälften, stellt ein Grundprinzip menschlicher Gehirnorganisation dar. Vor diesem Hintergrund ist es wenig überraschend, dass sich dieses Prinzip auch auf die Enkodierung von Gedächtnismaterial übertragen lässt. Einige Arbeiten beschäftigten sich bisher mit der Erforschung dieser Asymmetrie mittels funktioneller Magnetresonanztomographie (fMRT) vgl. (Golby, Poldrack et al. 2001; Golby, Poldrack et al. 2002; Powell, Koepp et al. 2005; Jansen, Sehlmeyer et al. 2009), ein Verfahren, dass sich den erhöhten Sauerstoffbedarf aktivierter Hirnareale zu Nutze macht, um Hirnaktivierung indirekt zu detektieren. Durch diese Studien wurden die Grundvoraussetzungen für die Annahme geliefert, dass verbalisierbare Informationen (z.B. Worte/Sprache) vor allem linkshemispherisch und schwer verbalisierbare Objekte (z.B. abstrakte Muster) vorwiegend rechtshemispherisch verarbeitet werden. Letztlich diente die Arbeit von Jansen et al. (Jansen, Sehlmeyer et al. 2009) als Vorläuferprojekt zu der vorliegenden Studie, in der zwei Stimulusklassen verwendet wurden und in der noch nicht auf Fragen der Reliabilität eingegangen wurde. Insgesamt wurden Fragestellungen der Reliabilität in der bisherigen Forschung nur vereinzelt behandelt vgl. (Bennett and Miller 2010), deshalb erschien es notwendig dieses in die vorliegende Arbeit zu integrieren.

Die vier Fragestellungen der Arbeit:

1. Die Implementierung des Paradigmas am neuen 3 T Scanner
2. Die Erweiterung des Paradigmas um zwei neue Stiumulusklassen
3. Entwicklung von weniger verbalisierbaren Stimuli
4. Reliabilitätsmessung durch Wiederholung der Messung und Vergleich der beiden Messzeitpunkte

Das Paradigma wurde erfolgreich am neuen Scanner etabliert. Durch die neuen Stimulusklassen (Szenen und Gesichter) konnten Zwischenstufen im Hinblick auf Verbalisierbarkeit zwischen den bestehenden gut verbalisierbaren und nicht verbalisierbaren Stimulusklassen (Worte und Muster), erstellt werden. Die neuen weniger verbalisierbaren Stimuli zeigten gute rechtslateralisierte Ergebnisse. Insgesamt konnten ähnliche Ergebnisse wie bei Golby et al. und Jansen et al. gezeigt werden. Die Reproduzierbarkeit der Ergebnisse zeigte sich jedoch nicht konstant gegeben. Die

verwendeten Verfahren zur Realibilitätsmessung, Intraclass-correlations (ICC) und Lateralisationsindices (LI), zeigten unterschiedliche Ergebnisse, wobei die LIs relativ gute Reproduzierbarkeit zeigten und bei den ICCs nur für einige selektive Cluster gute Ergebnisse erzielt werden konnten. Dies weist darauf hin, dass in Zukunft deutlich mehr Wert auf Reliabilität bei der Planung von fMRT Studien gelegt werden sollte.

Abstract

The concept of functional asymmetry is a basic principle of organization of human brain function. This basic concept also applies to the encoding of memory data. A number of studies have been conducted to explore the asymmetry of memory encoding using functional magnetic resonance imaging (fMRI), a technique which utilizes the high oxygen levels in activated brain areas to indirectly detect brain activation. The lateralization of encoding processes is determined, among other things, by the verbalizability of the memorized material (Golby, Poldrack et al. 2001; Golby, Poldrack et al. 2002; Powell, Koepp et al. 2005). Encoding of verbal stimuli preferentially relies on left-hemispheric brain regions, while encoding of visual (non-verbal) material relies on right-hemispheric areas. The study of Jansen et al. (Jansen, Sehlmeyer et al. 2009) was used as prototype study for this project, though only containing two stimulus classes and not addressing the issue of reliability. Reliability has only been addressed by a few studies (Bennett and Miller 2010), why we enclosed it into my study. The four objectives of this study are:

1. Implementations of the task at the new 3 tesla Siemens MRI scanner.
2. Expansion of the paradigm by two newly implemented stimulus classes
3. Development of stimuli with less verbalizeable patterns
4. Testing the reliability of the results by comparing it to a second run of the study

The establishment of the paradigm at the new scanner was successful. Through the inclusion of two additional stimulus classes (Scenes and Faces), to the existing classes (words and shapes), two additional steps between the existing very well verbalizeable and almost not verbalizeable, were established. The newly introduced almost not verbalizeable patterns showed, as expected, right lateralized activations. Overall similar results to those already published by Golby et al. and Jansen et al could be achieved. The reliability of the results was not entirely homogenous, since the two implemented techniques, the intra-class-correlations (ICC) and the lateralization indices (LI), showed deviating results. LIs resulted in a quite good reliability, but ICCs showed good reliability only for a few select activation clusters. This indicates that in the planning of future fMRI studies, reliability should be a key issue.

1 Introduction

Memory is an important part of everyday life. We all are dependent on it in every waking moment. Whether we converse with each other or we are on our own, our memory really makes us what we are. It defines us through the stored information of our experiences and things we learned. Without our memories we are totally lost and incapable of living our life and interacting with others. There would be no reference to refer to in conversation. Shared memories could not be revived. We would be living a life that comes from nowhere and leads nowhere.

Imagining different defects in memory function such as having no long-term memory, or having no short-term memory results in a different level of disability in everyday life. Either way the effects are devastating. Persons with loss of memory function are impaired in taking part in the social life around them and are often isolated. A movie produced in the year 2000 called "Memento" (http://www.imdb.com) took the viewer into the life of someone who had lost the ability to store new information in the long-term memory. The story is told backwards in little episodes starting from the end with each episode revealing a little more of the story. The protagonist, Leonard, is a former insurance investigator, who wants to solve the murder of his wife. The scene of his wife lying lifeless next to him is the last new information he was able to store in his memory. To substitute his broken memory, he uses Polaroid pictures to which he adds written notes, to remember people and places. Important information concerning his search for the murderers of his late wife, he tattoos onto his body. Throughout the film, it becomes more and more evident that Leonard uses different methods to assemble and interpret this puzzle of information, depending upon the situation. This leads him to suspect different people to be the murderer he is looking for and makes him subject to manipulation by other people. He is quite aware of his "condition" as he calls it and speaks freely about it. This leads to comic situations like the following one. He enters a bar and orders a beer. The barkeeper prepares the beer and he tells her about the memory state he is in. She puts this to a test and has some people sitting at the bar spit into the beer. Leonard notices this but after is attention is diverted for a little while, he gladly accepts the presented beer. This scene underlines how Leonard's memory condition makes him subject to manipulation. He is entirely dependent on the people

around him, to lead him in the right direction and to help him put what he has learned into a meaningful context. In the movie this results in a fatal error on Leonard's part. He wrongfully suspects the Police investigator Teddy (John) Gammell because he has the same first name and last name initials as the killer, as Leonard has them tattooed on his body: "John G.". In the end of the movie Leonard kills Teddy and the viewer finds out it was not the first "John G" Leonard has killed.

This entirely fictional movie shows in a very dramatic way the consequences of long-term memory malfunction. And this is exactly the scenario patients may face after epilepsy surgery where epileptogenic foci are surgically removed. Especially undergoing a common neurosurgical intervention called Amygdalohippocampectomy (Engel 1996). Due to the major role hippocampal structures play in declarative memory functions, results of surgery can be severe for memory function. In literature a famous patient named H.M. is often referred to when it comes to patients suffering from severe retrograde amnesia after undergoing epilepsy (Scoville and Milner 1957). This patient was one of the first ones on whom parts of the medial temporal lobe in both hemispheres have been removed to treat his epilepsy. This intervention reached its primary goal, the suppression of epileptic seizures, but produced severe anterograde amnesia. The patient was unable to transfer data into his long term memory. These observations were a major step towards a better understanding of memory functions. Nowadays, through many lesion and functional neuroimaging studies, the medial temporal lobe (MTL) is known as a critical structure for declarative memory encoding. For reviews see (Scoville and Milner 1957; Squire 1992; Gabrieli 1998; Eichenbaum 2000). The lateralization of encoding processes is determined, among other things, by the verbalizability of the memorized material (Golby, Poldrack et al. 2001; Golby, Poldrack et al. 2002). Encoding of verbal stimuli preferentially relies on left-hemispheric brain regions, while encoding of visual (non-verbal) material relies on right-hemispheric areas. In clinical diagnostic prior to neurosurgical interventions it is crucial to gain information about the functionality of the Hippocampus. Here different imaging techniques such as functional magnetic resonance imaging (fMRI) are used. FMRI has made it possible to study non-invasively the neural correlates of memory processes. In the clinical context, the technique is used increasingly in the pre-operative assessment of patients with MTL epilepsy since the anterior MTL is the major seizure

focus in epilepsy patients (Akanuma, Koutroumanidis et al. 2003). In many cases of medically refractory epilepsy, seizures can be controlled by neurosurgical removal of the seizure focus (Engel 1993). One side effect of MTL resection, however, is a decline in memory functions (Engel 1993). Thus, the benefit of anterior temporal lobotomy must be weighted against the risk of memory impairments. Measures of memory lateralization can help to assess the competence of the contra lateral MTL, and thus to decide whether or not to perform a surgery. Due to its high spatial resolution, fMRI also provides detailed information about the functional neuroanatomy of memory functions and thus can support decisions as to how far the resection of one MTL can be extended. Many research groups have therefore aimed to develop a comprehensive, clinically applicable fMRI test to assess hemispheric-specific, memory-related brain activation in the MTL (Jokeit, Okujava et al. 2001). A commonly applied memory task relies on the comparison of stimuli that are either "new", that is, shown only once during the experiment, or "old", that is, shown several times (Golby, Poldrack et al. 2001; Jansen, Sehlmeyer et al. 2009). Under the assumption that the encoding of known stimuli poses less demands on the neural network underlying memory functions, the comparison of both conditions enables to visualize brain regions that are involved in the encoding of information. Also called "novelty encoding"; for a discussion of other memory paradigms (Golby, Poldrack et al. 2001). The lateralization of brain activity depends on the verbalizability of the encoded material. The encoding of words typically leads to left-lateralized brain activity; the encoding of abstract patterns to right-lateralized activation (Golby, Poldrack et al. 2001).

To be clinically applicable, a memory paradigm has to fulfill a number of demands. First, it should be sensitive to the encoding of new information. Second, it should be applicable to patients in routine clinical settings. Third, the memory-related brain activity has to be assessable also in individual subjects, not only at a group level (Jansen, Sehlmeyer et al. 2009; Strandberg, Elfgren et al. 2011). Fourth, the brain activation must be reliable; that is, similar results should be obtained in repeated measurements. In particular for clinical questions, fMRI measures have to be sufficiently stable across measurements to assess differences in brain activity between subjects. If fMRI is used for surgical planning or clinical diagnosis, issues of reliability must be addressed.

Previous fMRI test-retest studies have assessed fMRI reliability for a range of paradigms, from basal sensory and motor tasks to more complex cognitive tasks. Overview in (Bennett and Miller 2010). According to Bennett and colleagues the results of group activation maps are often reproducible across measurements, while single subject activation measures are considered to be far less reliable. Motor and sensory tasks seem, in general, to have a greater reliability than task involving higher cognition such as memory (Bennett and Miller 2010). Relatively few studies, however, assessed test-retest reliability for memory tasks (Harrington, Tomaszewski Farias et al. 2006; Freyer, Valerius et al. 2009; Atri, O'Brien et al. 2011). These results are inconsistent. While some studies reported relatively high test-retest reliability related to memory encoding (Atri, O'Brien et al. 2011; Putcha, O'Keefe et al. 2011), others showed differing levels of reliability (Caceres, Hall et al. 2009). Given the central role of memory paradigms in the assessment of memory functions during the preoperative assessment of functional neuroanatomy, in the present study I specifically analyzed the test-retest reliability of fMRI brain activation related to memory encoding, with a specific focus on brain activity in the MTL. I used a commonly applied novelty encoding paradigm contrasting known and unknown stimuli. To be able to also assess brain lateralization, I used three different stimuli classes that differ in their verbalizability (word, scenes, and fractals). Test-retest reliability which of fMRI brain activation was assessed on the one hand by the intraclass-correlation coefficient (ICC), both on a voxel-by-voxel basis and a regions-of-interest (ROI) basis (Caceres 2008), on the other hand by examining the percent of subjects who showed reproducible activation within a given ROI (Harrington, Tomaszewski Farias et al. 2006). The retest was performed for 15 of the 20 subjects.

Objectives

This study aims to implement a paradigm to investigate the neural correlates of memory processes within the MTL. It is based on the already described original study of Golby and colleagues (Golby, Poldrack et al. 2001). They tried to establish a paradigm that predicts individual material-dependent memory lateralization (Golby, Poldrack et al. 2001). The hypothesis of this study was that different types of materials would activate memory encoding regions asymmetrically in dependence of their inherent quality to be verbalized. The prediction was verbal stimuli would activate left hemispheric regions

and visual (non-verbal) stimuli would activate right hemispheric regions preferentially. Also verbal encoding strategies have to be taken into account in accordance of the amount of left-hemispheric activation (Golby, Poldrack et al. 2001). The paradigm was composed of patterns, faces, scenes and words. Words were used as the verbal material and the other three categories as non-verbal stimulus material. An fMRI experiment was used to establish relative contributions of the left and right MTL and frontal regions to the encoding of the stimuli described (Golby, Poldrack et al. 2001). This study showed good results in group level analysis and some results for chosen individuals.

Brain activations from earlier shown "old" stimuli were compared to those resulting from entirely new pictures. Golby and colleagues were able to show a stimulus-dependent lateralization on group level and some on single subject level.

A previous study in our workgroup was carried out by Sehlmeyer (Jansen, Sehlmeyer et al. 2009) and used only two stimulus categories: words and abstract patterns. Entirely new stimuli were created. Again, good results, including the expected lateralizations were achieved on group level, but for the single subject level, consistent results could not be noted.

The results of these two studies lead us to the objectives of the study at hand.

1. Implementations of the task at the new 3 tesla Siemens MRI scanner.
2. Expansion of the paradigm by two newly implemented stimulus classes
3. Development of stimuli with less verbalizeable patterns
4. Testing the reliability of the results by comparing it to a second run of the study

Layout

In the following, the structure of the thesis is described.

The second chapter "Theoretical and Methodical Basics" gives an introduction to the methods used and the theoretical background needed. At first memory basics and lateralization are described and explained. After that follows a short look into the hippocampus and its significance for memory functionality. Following theoretical basics of magnetic resonance imaging (MRI) and fMRI are laid out and used techniques are shown. At last in this chapter, the statistical analysis applied in this study is explained.

The third chapter "Methods" includes the paradigm adapted for this study, the experiment undertaken is presented in detail, the paradigm is explained and the data analysis implemented is presented.

The fourth chapter "Results" presents the fMRI data for group level, plus the reliability data is displayed.

The fifth chapter "Discussion" holds the analysis of the data produced in this study, the implications drawn from that and the outlook on future research.

2 Theoretical and Methodical Basics

In the following, I give an overview about the theoretical background that is important for the present study. I start with a short introduction on the classification of memory functions (2.1), describe the important role of the MTL in the memory system (2.2), and give an overview how MRI techniques can be used to analyze brain activity (2.3.-2.5).

2.1 Memory Functions

In general the human memory can be described as three different systems, which have different storage times. These systems are the sensory memory, the short-term memory and the long-term memory.

2.1.1 Sensory Memory

According to Deetjen and colleagues the flow of sensory information comes from the sensory organs to the sensory memory. The storage capacity is rather spacious and is 10^6 in the acoustic memory and 10^7 bit/s in the optic memory. The information is stored in the sensory memory for about 0.5 to 1 second. After that time information fade or are completely lost. Storage time depends on the intensity of the sensory stimulus. In the sensory memory, information is compared to already existing in other memory parts and valued to their global significance. This allows selective turns of attention to potentially dangerous stimuli. Also, are information newly encoded, for example into words (verbalization) (Deetjen, Speckmann et al. 2005).

2.1.2 Short-Term Memory

From the sensory memory the now redundancy-cleaned data is transmitted to the short-term memory. The speed of this transmission is only 16 bit/s. The short-term memory is also called the primary memory. Its storage time is longer compared to the sensory memory and ranges from seconds to minutes. Storage times of minutes are reached, for example, if verbal information is repeatedly repeated in thought. Memory capacity is estimated at a couple hundred bits. This is much less than the sensory memory. Only up to seven items can be stored at one time. These items are called chunks. Each of these chunks usually holds more than 7 bits consisting of letters, words, or numbers. Through this process called chunking it is possible to extend the capacity of the short-term memory (Deetjen, Speckmann et al. 2005).

2.1.3 Long-Term Memory

Since items in the working memory are lost by overwriting, repeating is necessary to manage transfer to long-term memory. The maximal transfer speed is 1 bit/s. Long-term memory has a large capacity of 10^{10} to 10^{14} bit to store items for month up to decades. Access time to data stored in a secondary memory may be quite long (Deetjen, Speckmann et al. 2005). Data inside the long-term memory can be deleted by earlier or later encoded data. Most likely to be deleted are memory items which are either of low significance, have not been accessed for a long time, or were encoded in a state of low motivation.

A tertiary memory can be identified inside the long-term memory. This tertiary memory includes data that is used on a day to day basis and is not deleted as long as the memory is intact (Deetjen, Speckmann et al. 2005).

Psychological studies have shown that long-term memory qualities can be differentiated by memory content and function. Two different parts can be identified as procedural memory and declarative memory. Procedural memory is available even in early childhood whereas declarative memory is not fully functioning until the 4th year of life.

Priming, which is included in the procedural or implicit memory, is a pre-conscious memory which is used to recognize before seen sensory information even if they are only slightly related. In adulthood, this is used to complete incomplete words or pictures. Procedural memory is also available in early childhood. Data about learned procedures like bicycle riding or car driving is stored here.

The semantic memory is part of the declarative memory. Its content consists of explicit terms and its meanings, such as the capital of Germany is Berlin. The semantic memory also holds meanings of symbols and signs. The second part of the declarative memory is the episodic memory. Memories of personally-experienced episodes with defined place and time are stored here, such as recollections of a wonderful party.

The difference between declarative and procedural memory is that declarative memory is stored in verbalized form. In contrast, procedural memory is stored in non-verbalized, non-explicit form. Procedural memory is stored more securely and is sustained for decades. This leads to the conclusion that different memory types are stored in different anatomical areas.

Even though data is stored in the memory, its storage is not static. Changing opinions or

changing ways of thinking can change the perception and interpretation of memory content (Deetjen, Speckmann et al. 2005).

2.1.4 Memory Localization

Short-term memory is one of the important functions of the prefrontal cortex but also other cortical areas seem to contribute their share (Trepel 2008). The long-term memory is located in the cerebral cortex. Aside from the association cortex also the secondary auditory cortex, the motor cortex, the optical cortex and other parts of the cerebral cortex are part of the long-term memory network (Trepel 2008).
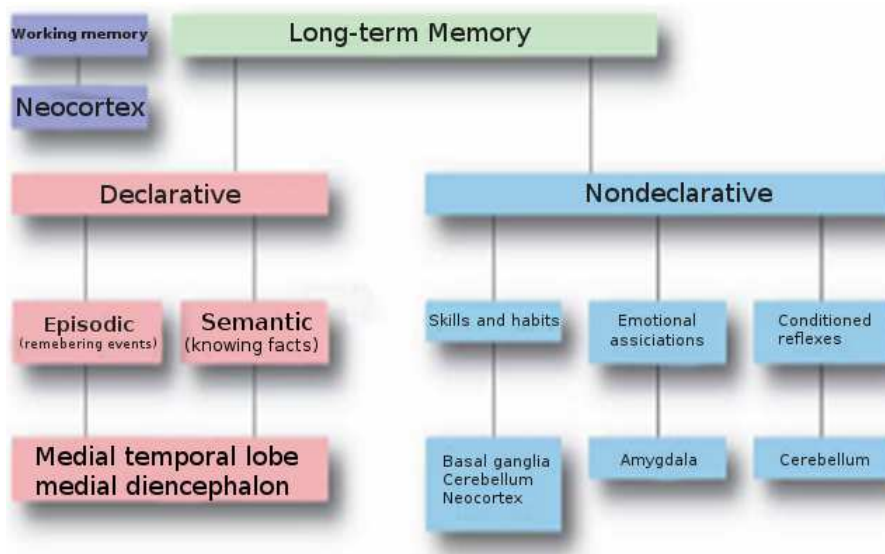
Figure 1 Memory localization adapted from (Nolte 2009)

Figure 1 illustrates the memory localization. Declarative part of long-term memory is located in the medial temporal lobe and the medial diencephalons. This was also the area of main focus in the present study. The non-declarative (or procedural) memory is stored in different areas depending on their quality. Skills and habits are stored in the basal ganglia, the cerebellum and the neocortex. Emotional associations are stored in the amygdala and conditioned reflexes are stored in the cerebellum (Nolte 2009). Since the experiments in this thesis are to be classified as declarative memory tasks, the medial temporal lobe, in particular the hippocampus, were chosen as regions of interest.

2.1.5 Memory: Hemispherical Dominance

Lateralization describes the asymmetry of brain tasks. For most of these tasks both hemispheres are used but one hemisphere usually dominates. As early as 1844, Arthur Ladbroke Wigan published a book *A New View of Insanity: Duality of Mind* in which he described the hemispheres as separate systems of volition and mental activity. According to his view, in a sane person, the dominant hemisphere was in control. In case of a mental illness the hemispheres would have contrary volition and mental activities. (Wigan 1844)

As Sören Krach pointed out, in 1836, the physician Marc Dax realized that all of his patients with language production dysfunction had suffered from left hemispherical strokes. Without knowledge of Dax's work, Paul Broca published in 1864 nine autopsies of aphasic patients who showed only left hemispherical lesions. These were the first scientific clues to functional hemispheric asymmetry. The left hemisphere was called the language dominant hemisphere and the right one the non language dominant hemisphere. Today neuroimaging techniques and field of vision techniques are also used on healthy subjects to complement studies with brain damaged patients. It is important to understand that hemispheric specialization is only to be seen as hemispheric dominance. Any given task is most likely not carried out by a single hemisphere as was believed before. Today it is perceived that the different hemispheres participate to a certain degree in different cognitive tasks (Krach 2006).

Lateralization of the brain activation is a crucial part of this work which I examined throughout three different paradigms containing three different stimuli classes. According to Golby et al. as verbalization of the stimuli increases, lateralization of brain activation moves increasingly to the left hemisphere (Golby, Poldrack et al. 2001).

2.2 Memory Functions and Hippocampus

Anatomically, memory functions are associated with a large-scale neuronal network. Within this network, in particular the hippocampus plays a crucial role. According to Nolte and colleagues, it was discovered in the 1950s by accident that the removal of the median parts of the medial temporal lobe resulted in an almost complete anterograde and some retrograde amnesia. Patients were not able to encode new information. As soon as their attention was lost, they lost any new information given. Some events right before the surgery were also lost, but early memory was functioning. The patients

remained generally at their normal intelligence level. Only declarative amnesia was suffered by the patients; the learning of skills and procedures was intact. The hippocampus has therefore been identified as a key structure with the function of encoding and consolidating new memories (Nolte 2009).

2.2.1 Anatomy

The hippocampus is part of the limbic system. Cinguli gyrus, parahippocampal gyrus, entorhinal area, amygdala and the mamillary body are the remaining parts of the limbic system. It has been identified as the source of emotion in the human brain, for visualization see figure 2 (Trepel 2008).

The hippocampus is localized in the temporal lobe next to the medial wall of the side ventricle. A paw-like part, called pes hippocampi, forms one end of the hippocampus structure. The hippocampus reaches back to the caudal end of the corpus callosum. Cranial the fornix of the hippocampus, runs ventral under the corpus callosum. Further ventral, the fornix arches over the third ventricle and ends in the mamillary bodies (Trepel 2008).

Anatomical position of the hippocampus and the fornix inside the hemispheres

1 hippocampus pes hippocampi, 2 gyrus dentatus, 3 crura fornicis, 4 commissura fornicis, 5 corpus fornicis, 6 columnae fornicis, 7 corprora mamillaria, 8 posterior horn of the side ventricle, 9 corpus callosum, 10 sulcus centralis, 11 fissura longitudinalis cerebri
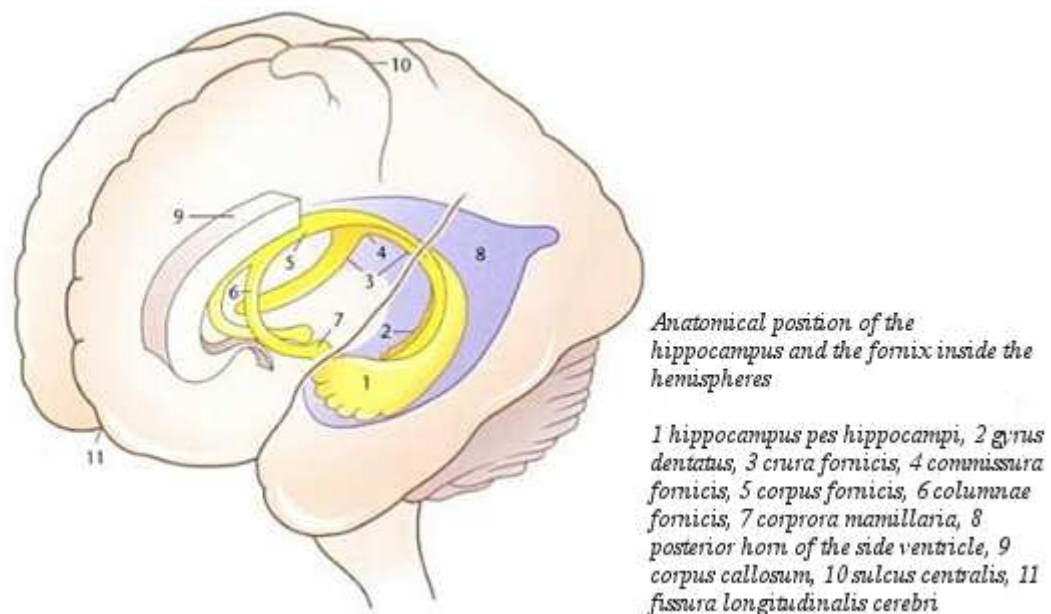
Figure 2 Adapted from (Trepel 2008)

The hippocampus has according to Trepel and colleagues (Trepel 2008), numerous afferences from the entorhinal area inside the parahippocampal gyrus. These afferences originate in the piriform cortex, the amygdala and the neocortex. Their quality is

sensory, visual, auditory and olfactory. Further afferences originate in the thalamus, the cinguli gyrus and the septum region.

Efferences of the hippocampus are almost entirely localized in the fornix region. Some fibers leave the fornix on their way to the septum, the amygdala and the hypothalamus. Most of the fibers run to the mamillary body and form the so-called Papez circuit. This circuit runs from the hippocampus to the mamillary bodies, from there to the nucleus anterior of the thalamus and to the cinguli gyrus. From there, some fibers continue to the hippocampus. A variation of the Papez circuit, with added connections to the parahippocampal gyrus, seems to play a significant role in the transfer of data from the short-term memory to the long-term memory (Trepel 2008).

2.3 Magnet Resonance Tomography (MRI)

Magnet resonance tomography (MRI) is a highly sophisticated non-invasive imaging technique that can be used to visualize the structures of the human body typically viewed as cross-sections. The technique has been developed in the beginning of the 1970s and is today mainly used for diagnostics in the clinical routine. Physical background of the MRI is the phenomenon of nucleus spin resonance. Hydrogen nuclei, which are present in the human body mainly as water, have a so called spin, or spinning impulse. Derived from that is a magnetic couple of force. Through the effects of a strong outer magnetic field these couples of force are aligned either parallel or antiparallel to the outer field. Since the parallel alignment is energetically favorable most atomic nuclei assume this alignment. This results in a magnetization of the body, which lies inside the tomograph to be examined. Modern MRIs use superconducting coils to generate the magnetic fields. Field strength lies in the general order of 1.5 to 3.0 tesla for clinically used tomographs. The magnetizing of the examined body can be changed by applying an alternating magnetic field which oscillates orthogonal to the outer magnetic field. This alternating magnetic field has to be oscillating in a suitable frequency also called Lamor's frequency. This frequency is depending on the strength of the outer magnetic field. Through the effects of this additional magnetic field the examined body receives energy which results in a change of his magnetization. After the alternating magnetic field is shut down, the magnetization of the body resumes to its primary condition. This process is called relaxation. Through relaxation the beforehand acquired energy is emitted in form of radio waves. The emitted radio waves can be

detected by detection coils. The temporal dynamic of this relaxation process is dependent amongst other things on the tissue of the body; therefore from the detected radio waves conclusions about the anatomy of the examined body can be drawn. By combining additional magnetic fields, overlaying the outer magnetic field the consistency of the tissue of the examined body can be examined in a high resolution cross section. A showcase image can be seen below in figure 3. For further information please see "MRI made Easy" by Schering or "Magnete, Spins und Resonanzen – Eine Einführung in die Grundlagen der Magnetresonaztomographie" (2003) by Siemens.

Figure 3 Showcase MRI image (Image by Ranveig; published under GPL)

2.4 Functional Magnet Resonance Tomography (fMRI)

Functional magnetic resonance tomography (fMRI) is a specific application of MRI. Through this technique, physiological functions of the body, especially brain activation during certain tasks can be examined.

2.4.1 Physical Basics of fMRI

The execution of specific tasks results in higher neuron activity in designated brain areas. Through neurovascular coupling, neuron activation results in higher metabolism activity in the associated brain area. Oxygen levels decrease at first, but are overcompensated by a higher blood flow. This results in a higher oxygen level in activated neural areas (Fig. 4).
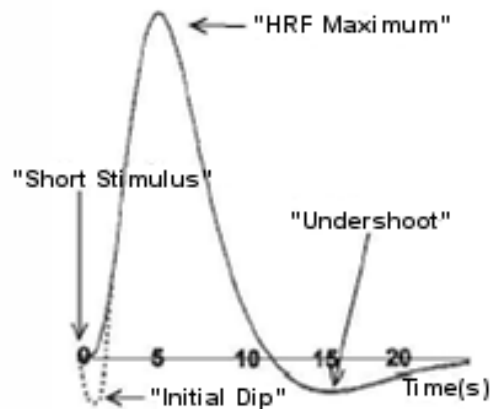
Figure 4 Curve of BOLD-Signal as registered after a stimulus. Showing an initial dip in the oxygen level with a maximum at roughly 5 seconds and a following undershoot. Adapted from (Jansen 2004)

In the most common case fMRI is used to compare brain activity between two task conditions, an activation condition (e.g. movement of the right hand) and a controlling condition (e.g. resting). As stated before in both conditions the oxygen levels differ. In the activating condition more oxygenated hemoglobin is to be found in the neural active area than in the controlling condition. Oxyhemoglobin and desoxyhemoglobin show different magnetic characteristics. Oxygenated hemoglobin is diamagnetic, not oxygenated hemoglobin is paramagnetic. This results in different relaxation times between the two conditions, effecting in detectable signal changes of the MRI. Through this process it is possible to monitor physiological changes via MRI. This effect is called blood oxygen level dependent (BOLD) effect.

The spatial resolution of a typical fMRI study is around 3x3x3 mm, but nowadays higher resolutions are possible. Temporal resolution of fMRI is just around 2 seconds. It has to be taken into account that in comparison to other electrophysiological techniques (e.g. EEG, magnetoencephalography (MEG)) immediate conclusions to the underlying neurological response are limited because of the inertia of the blood flow response (Knecht, Jansen et al. 2003). For more information regarding fMRI see also (Heeger and Ress 2002)

2.4.2 Value of functional Magnetic Resonance Tomography

The BOLD signal is only an indirect measurement of neural activity. Therefore, the fact that the BOLD signal consists of the sum of many activated neurons has to be taken into account. The BOLD signal can result from a small number of highly activated neurons

or a large number of relatively weak activated neurons (Heeger and Ress 2002; Krach 2006). FMRI has a weak time-resolution because, as indicated before, the haemodynamic response to neural activity is slower than the neural activity it depends on. Other methods such as functional transcranial Doppler sonography (fTCD) or EEG have a much better timely resolutions. The lumen of the arteries and capillaries supplying the examined region cause certain variability of the BOLD signal as suggested by Krach. (Krach 2006) Larger arteries cause a stronger signal, but are usually located some millimeters from the neural activity. The spatial resolution is negatively influenced as a result of this effect (Krach 2006).

2.5 Data Analysis

In the present study, fMRI data was analyzed using the SPM software package Version 8 (SPM 2009). Analysis consists of three steps: spatial preprocessing of the data, statistical analysis and statistical interference (Fig 5).
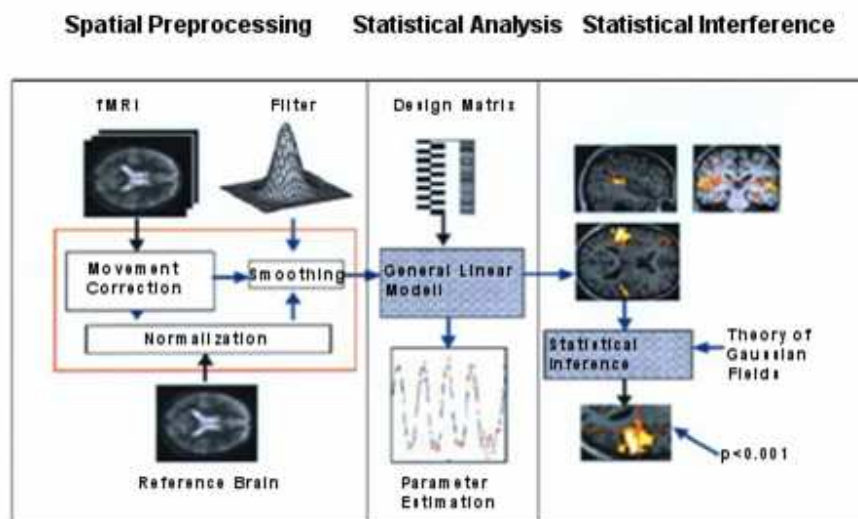
Figure 5: Three steps of Data Analysis. Adapted from (Sehlmeyer 2006)

2.5.1 Spatial Preprocessing

Spatial preprocessing typically consists of at least three steps: correction for movement artifacts (called realignment), normalizing of the data to a standard brain and smoothing. Realignment: during the scanning movement of the subject is inevitable. Even minimal movement can result in signal change which might be more powerful than the signal change induced by the change of tasks. Because of this, as a first step a mathematical correction has to be applied, which corrects for these movement artifacts to the greatest

possible extent. To achieve this all recorded images are transformed to match the first recorded image.

Normalizing: the second step of the preprocessing is the normalization of the data. In this step all recorded images are transformed into a so called standard Brain ("MNI-Brain"). Through the process of normalization especially size and form of the individually recorded brains are changed to fit into the used standard brain to the greatest possible extent. Through normalization the recorded data of different subjects are averaged. Only through this step it is possible to compare activations of a group of different subjects as well as differences between groups. Furthermore it is possible to localize activations using a standardized databank.

Smoothing: the last step of preprocessing is spatial smoothing of the data. This typically results in an increase of the signal-noise-ratio. The smoothing is usually processed using a Gaussian filter. The optimum filter size is determined by the size of the underlying activation.

2.5.2 Statistical Analysis

There are different methods of statistical analysis of functional MRI data. These methods can be differentiated by their aim. In order to relate cognitive, motor, or sensor functions to anatomical structures the location of the physiological signal is analyzed. Since this is the only method used in this thesis other analysis methods (for example connectivity analysis) will not be furtherly considered.

The analysis software SPM is based on linear parametrical mapping methods which are based on the general linear model (Friston 1995c). These methods are used to find significant associations between the experimental variables and the observed signal. The data analysis approach is univariate, that is, an a-priori hypothesis is tested for every voxel in the brain.

The experimental variables are specified at the beginning of the data analysis in a so called design matrix. This matrix contains information about the chronological parameters of the experiment, but also influencing variables such as movement parameters. The recorded signal for each voxel is compared to the design matrix. The relationship of the recorded signal and the sequence parameters in the design matrix for each voxel are expressed as a statistical t-value (Fig. 6).
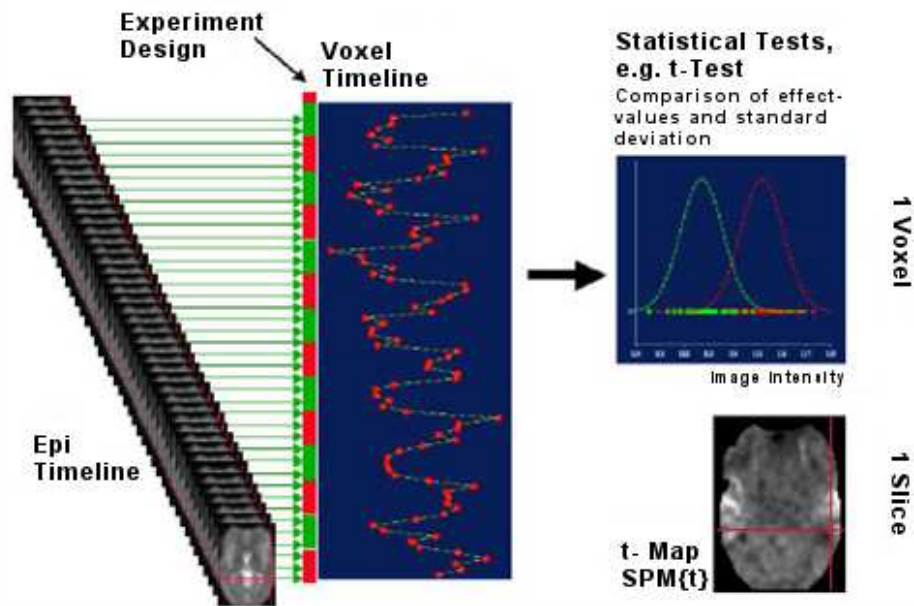
Figure 6 t-map. Adapted from (Jansen 2004). Each voxel recorded over the course of the functional time course and its relationship to the design matrix is expressed in a statistical t-value and then plotted in a t-map.

2.5.3 Statistical Inference

As the third step, the statistical inference, on the basis of the beforehand computed t-maps it is evaluated which voxel can be assessed as "active". For this, a threshold value (p-value) is defined. Typically threshold values of statistical tests lie at p=0.05. But it has to be taken into account that fMRI data is multidimensional. Taking 100.000 voxels of the brain at a threshold of p=0.05, 5000 voxels would be wrongfully considered active. To correct for these errors adequate corrections have to be applied, such as using the theory of Gaussian fields. For further information see Worsley and colleagues. (Worsley, Marrett et al. 1996)

2.5.4 fMRI Lateralization Index Analysis (fMRI-LI)

Lateralization of brain activation can be expressed using a so called lateralization index (LI). The LI is calculated as follows:

$$LI= (L-R) / (L+R),$$

where L stands for the activations of a defined region of the left brain hemisphere and R stands for the activation of the homologue region of the right hemisphere. The LI can range from -1 to 1. A value of +1 marks exclusively left dominant activation and a value

of -1 an exclusively right lateralized activation.

There are different ways to calculate the extent of activations (for an overview see (Specht, Willmes et al. 2003; Kloppel and Buchel 2005; Branco, Suarez et al. 2006; Jansen, Deppe et al. 2006). In this thesis the LI is calculated by the number of activated voxels in the chosen regions of interest. Since this number fluctuates greatly in dependence of the statistical threshold p all LI values are calculated for different p-values.

2.5.6 Intra-class Correlation (ICC)

There are different ways to describe the reliability of brain activity. For an overview see (Bennett and Miller 2010). In the present thesis, I applied an intra-class correlation coefficient (ICC) which sets within-subject variance (σ^2_{within}) in relation to between-subject variance ($\sigma^2_{between}$). According to Shrout et al., there are many different ways of calculating ICCs (Shrout and Fleiss 1979). The one used here is to be described as an intra-class correlation, which is calculated between two different time cluster values ("ICC(3,1) type"). The ICC is typically computed taking the ratio of the variance in focus divided by the total variance (Bennett and Miller). The formula for ICC 3.1 can be stated as follows: $ICC = \sigma^2_{between} / (\sigma^2_{between} + \sigma^2_{within})$ adapted from (Bennett and Miller 2010).

The ICC used in this study was computed as a whole-brain analysis using the ICC toolbox created by Alejandro Caceres (Caceres 2008). As pointed out by Bennett et al., this is the strictest method of measuring reliability (Bennett and Miller 2010).

3. Methods

In this chapter the experimental methods used in this study will be described in detail. The paradigm was taken and modified from the studies of Golby and colleagues (Golby, Poldrack et al. 2001) and Jansen and colleagues (Jansen, Sehlmeyer et al. 2009). As stated in these studies, the task was designed to stimulate activation in the medial temporal lobe. Non-verbal stimulus material was chosen in accordance to its verbalizability to explore material specific lateralization in MTL activation.

In the following, first the paradigm (3.1) is described, and then the experimental procedure is explained (3.2) and finally how the MRI data was analyzed is described (3.3).

3.1 Paradigm

The general idea of the paradigm aims to trigger the encoding process in each subject's brain, specifically the medial temporal lobe and to register the resulting activation using the fMRI technique. To achieve this, two different conditions were created and presented in an alternating two block design. These conditions were defined as "old" and "new". The condition "old" contained stimuli that were already shown ten times each, earlier in the experiment, while the condition "new" included stimuli that had never been shown before. The encoding load is much higher for new stimuli than for old ones; therefore the contrast of these two conditions was used to register the encoding activation. As was shown by Golby and colleagues (Golby, Poldrack et al. 2001) the contrast of these different activations in areas like the prefrontal cortex or the medial temporal lobe is associated with encoding processes.

The paradigm included four different stimuli groups. These groups included words, color photographs of faces on an even background, color photographs of indoor and outdoor scenes, and colored as well as black and white fractals. These groups were chosen in accordance to their differing verbalizabilities (words>scenes>faces>fractals), to examine activation in dependence of verbalizability. To focus the attention of the subjects on the stimulus material, a dichotomic dummy task was implemented for each stimulus group. In the words group, for instance, subjects were asked to differentiate nouns and verbs. Each group of stimuli was shown in a separate session. Prior to the scanning, subjects were instructed to watch a series of the 10 stimuli of the "old" group

each shown ten times. After a following short written instruction the corresponding task appeared on the screen.

In the following, the stimulus material is described in more detail (3.1.1) and explained how the stimuli were presented (3.1.2).

3.1.1 Stimulus material

Four types of stimuli were presented to each subject in separate sessions. The first group of stimuli contained colored and black and white fractals. These fractals were created using Apophysis 2.02 for Linux, licensed under general public license (GPL) by Peter Sdobnov, Piotr Borys and Ronald Hordjk (http://apophysis.org/index.html). All pictures were scaled to 354x354 pixels and 50 percent were converted to black and white using Irfanview 4.25 for Microsoft Windows®, Copyright by Irfan Skiljan (http://www.irfanview.de/). The task assigned to this paradigm was to differentiate between the colored and the black and white pictures. Below are some example images.

Figure 7 Fractals: An example of a coloured fractal
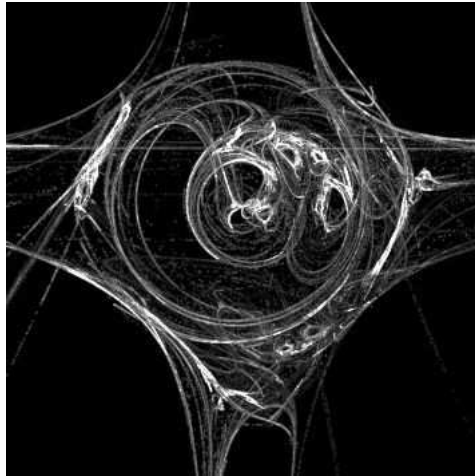
Figure 8 Fractals: An example of a fractal held in black and white

The second group of stimuli consisted of words. We used German nouns and verbs with medium word frequency in the German language as indicated in the Celex Word Database of the Max Planck Institute for Linguistics in Nijmwegen (http://www.ru.nl/celex). The words used had 2 syllables and were 4-7 letters long. Half of the words were verbs, the other half nouns. Words were presented in black capital letters on grey background (Fig. 9 and 10). To ensure a high level of attention, the participants were instructed to indicate whether a presented word was a noun or a verb. The words used in this paradigm were mostly taken from Jansen's study (Jansen, Sehlmeyer et al. 2009). They had been tested and validated in that study. Additionally, needed words were also taken from the Celex Word Database of the Max Planck Institute for Linguistics in Nijmwegen. Using a simple software tool written by Dr. Jens Sommer (Department of Psychiatry, University Marburg), the words were converted into images size 354x354 pixels with black capital letters on grey background to match the other stimulus material.

Figure 9 Words: An example of a noun on grey background used in the words paradigm

Figure 10 Words: An example of a verb on grey background used in the words paradigm

The third group of stimuli consisted of photographs of indoor and outdoor scenes. The images used were collected from private and internet sources, e.g. http://www.hintergrundbilder-pc.de/, http://www.flickr.com/ (see Fig. 11 and 12). The photographs were also resized to 354x354 pixels. Half of the photographs depicted indoor scenes, the other half outdoor scenes. The task assigned was to indicate whether these pictures showed indoor or outdoor scenes.

Figure 11 Scenes: An example indoor scene used in the scenes paradigm
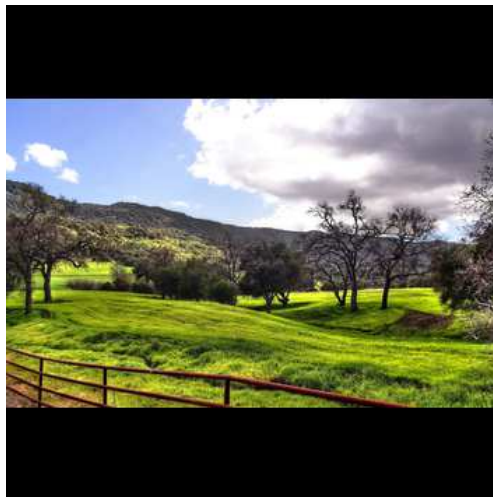
Figure 12 Scenes: An example outdoor scene used in the scenes paradigm

The fourth group of stimuli included color photographs of faces. These photographs were taken from a database produced by Minear in Dallas (Minear and Park 2004) showing equal numbers of men and women of different ages with neutral mimic (see Fig. 13 and 14). Faces were shown on grey background and the clothing was covered by a darker grey silhouette. The task assigned here was to differentiate between males and females. Images were resized to 354x354 pictures and included into the stimulus material.

Figure 13 Faces: An example of the female stimulus class used in the faces paradigm
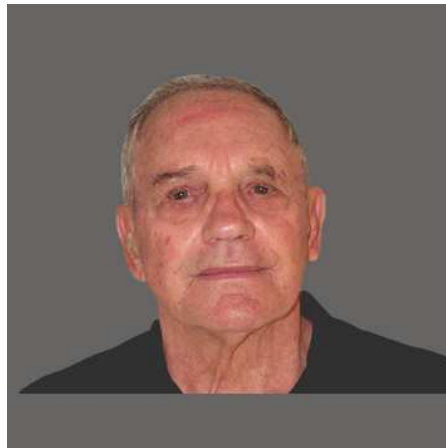
Figure 14 Faces: An example of the male stimulus class used in the faces paradigm

3.1.2 Stimulus presentation

The four types of stimuli (fractals, words, faces, scenes) were presented to each subject in separate sessions. The timing of the stimulus presentation was identical for each stimulus category. The order of stimulus class presentation was counterbalanced across subjects.

Each session consisted of two trials: an introductory trial and a main trial. In the introduction, familiarization took place by showing ten stimuli earlier described as "old" ten times for two seconds each. The main trial consisted of alternating blocks of variable length of either "old" stimuli already shown in the introduction, and "new" stimuli, not seen before in this experiment. Block sizes varied from two to six stimuli with an average length of 5 and were pseudo-randomized beforehand. Stimuli were presented for 2 seconds followed by a fixation cross shown for 2 seconds (see Fig. 15). To ensure high levels of attention, subjects were given a material-specific task which

consisted of verb/noun-decision in the verbal paradigm, male/female-decision in the face paradigm, indoor/outdoor-decision in the scenes paradigm and colored/non-colored-decision in the fractal paradigm. Responses were only recorded while the picture was shown. For each paradigm 24 blocks were shown containing a total of 66 images.
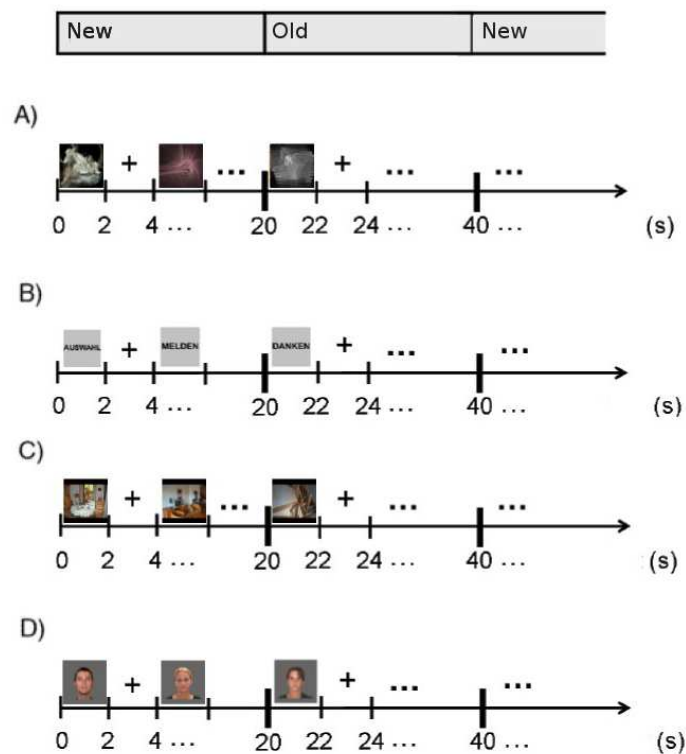
Figure 15 Adapted from (Sehlmeyer 2006): An example of the layout of the main trial of the following paradigms: A) fractals, B) words, C) scenes, D) faces. Stimuli are shown alternating with fixation crosses in each block. Old and new blocks alternate also. The main trial was shown after the introductory trial as stated above

3.2 Experiment

In the following the experiment will be described in more detail. Subjects' characteristics (3.2.1), the experimental procedure (3.2.2) and the MRI data collection (3.2.3) will be described.

3.2.1 Subjects

Twenty healthy subjects (13 men), aged 20 – 37 years (mean age = 25.6 standard deviation = 4.0 years), participated in the study. Written informed consent was obtained prior to participation according to the declaration of Helsinki. The study was approved

by the Ethics committee of Medical Faculty of the University of Marburg. All participants were native German speakers, right-handed according to the Edinburgh handedness inventory (Oldfield 1971) and had completed the equivalent of a high school degree ("Abitur"). None of the subjects had a history of neurological or psychiatric illnesses, brain pathology or abnormal brain morphology in T1-weighted MR images. To investigate the test-retest reliability, subjects were scanned during two sessions separated by 35 days on average (standard deviation: 11 days; range 20–57 days). 5 participants were not available for a second measurement.

3.2.2 Experimental procedure

Before entering the fMRI control room subjects were informed about the test. Their personal data was taken. The written consent was obtained. Possible contraindications for the participation in this study were ruled out (e.g. metal implants, pregnancy).

Handedness was estimated by an abbreviated version of the Edinburgh Handedness Inventory (Oldfield 1971). This test estimates subjects' handedness by an index calculated by the number tasks the subjects perform with their right hand out of a given list of tasks. The tasks included: Writing, drawing, throwing, using scissors, brushing teeth, using a knife, using a spoon, using a broom, lighting a match and opening a box. The index ranges from -1 to +1. Results of -1 indicate an almost absolute left handedness and +1 indicate an almost absolute right handedness. Subjects reaching at least +0.30 were classified as right handed and were accepted into the study.

The subjects were instructed to watch the stimuli presented to them closely and to answer a trivial question for each stimuli. They were intently not told to memorize the pictures. It was not disclosed to them that the task at hand was a memory task. They were instructed to respond with button presses using a five key keyboard which was attached to their right leg during the scan.

After the MRI measurement (see 3.1 for a thorough description), the subjects had to perform a recognition memory test outside of the MR scanner, in which for each stimulus class the same 60 new stimuli were randomly presented along with 60 other distractor stimuli that were not presented before. The subjects were instructed to indicate via mouse click whether they had seen the images during the fMRI scan or not. The layout of the trials resembled the one used in the main experiment. Stimuli were shown for 2 seconds followed by a fixation crosshair for 2 seconds. The different

stimuli classes were retrieved in the same order as they were shown in the main experiment.

3.2.3 MRI data collection

MRI data was collected on a 3T Tim Trio MR scanner (Siemens Medical Systems, Erlangen) at the Philipps-University Marburg. A standard head coil was used. To lessen movement of the head during the scan the subjects' heads were tightly cushioned with foam wedges. Before the actual experiment, an anatomical T1-weighted MR image was taken. This image was later burned onto a CD and given to each subject after participating in the study. A five key keypad was attached to their right leg to enable the subjects to respond to the task.

The functional images were collected with a T2* weighted echo planar imaging (EPI) sequence sensitive to BOLD contrast (64×64 matrix, FOV 230 mm, in plane resolution 3.6 mm, 36 slices, slice thickness 3.6 mm, TR=2.25 s, TE=30 ms, flip angle 90°). Slices covered the whole brain and were positioned transaxially parallel to the anterior–posterior commissural line (AC–PC). In total, 330 functional images were collected in each session. The initial 115 images measured during the instruction trials in which the "old" stimuli were repeatedly presented (see 3.1.2) were excluded from further analyses. The stimuli were presented either on a LCD screen or on video goggles using the software package "Presentation" (NeuroBehavioural Systems Inc.). The LCD Screen located behind the MRI scanner was viewable via a little mirror placed on top of the head coil. For subjects with impaired vision video goggles with adjustable acuity were used instead, to display the stimuli sustaining good visibility.

3.3. fMRI Data Analysis

SPM8 standard routines and templates were used for fMRI data analysis. During preprocessing, the functional images were realigned, normalized (resulting voxel size 2 x 2 x 2 mm^3), smoothed (applying a 8 mm full-width-at-half-maximum, FWHM, isotropic Gaussian filter), and high-pass filtered (cut-off period 128 sec).

Statistical analysis was performed in a two-level, mixed-effects procedure separately for each stimulus material and each measurement. At single subject level, BOLD responses for the encoding of new and old stimuli, respectively, were modeled by the canonical hemodynamic response function of SPM8 and its time derivative. The timing

parameters of both conditions were extracted for each subject from their Presentation log files using a software tool called "DataWeasel" (Ruprecht 2009). Besides the onsets of both conditions, the six realignment parameters of head motion were also included in the statistical model to account for residual head movement. An example design matrix is shown in figure 16. Contrasted parameter estimate images (con-images), describing brain activation differences between new and old stimuli ("new > old"), were calculated for each subject using the SPM contrast manager. To achieve this, the column in the design matrix holding the "New" blocks was set to 1 and the one containing the "Old" blocks was set to -1. These con-images held the information of signal changes between the "New" and the "Old" blocks.

At the group level, one-sample t-tests were conducted separately for each session with the con-images as input data to identify brain activation related to memory encoding. Anatomical localization of brain activity was assessed using the WFU-PickAtlas (http://fmri.wfubmc.edu/software/PickAtlas) and the SPM Anatomy Toolbox (http://www.fz-juelich.de/SharedDocs/Downloads/INM/INM-1/DE/Toolbox/Toolbox_18.html).
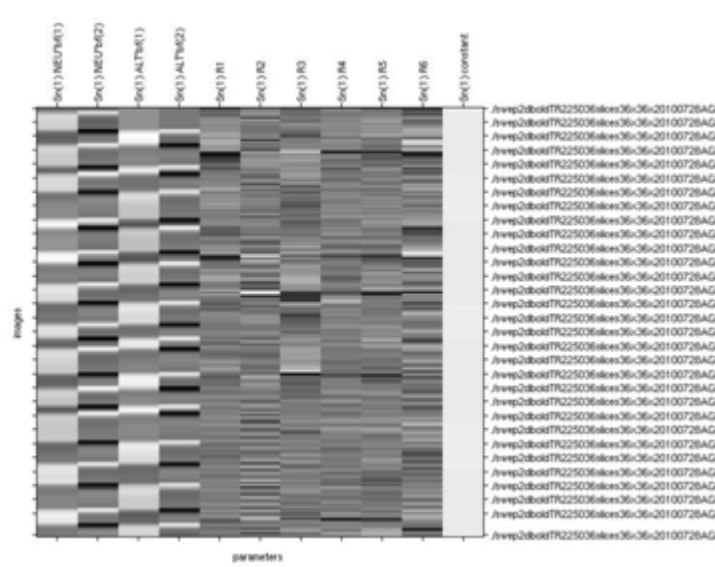
Figure 16: Design Matrix. The figure shows an example design matrix taken from the actual study data. Task blocks are represented in the first and the third column whilst the second and fourth columns show the results of the time derivative calculation. Movement data generated in the preprocessing is represented in the following six columns.

3.3.1 Presentation of results

The results were assessed in two steps. First, brain activity was analyzed on the group level separately for each paradigm. The main question was if it is possible to detect brain activity in the MTL. Both a whole brain analysis and a ROI analysis of the MTL were performed.

Brain activity in the MTL was expected for all four paradigms for the contrast "new > old". Analogous to the results of Golby and colleagues (Golby, Poldrack et al. 2001), we expected left-lateralized brain activity of the MTL for the verbal stimuli, right-lateralized activity for the fractals, and bilateral activity for both faces and scenes. Activation analysis for the whole brain was performed using a grey matter mask. This mask was created with the help of the WFU-Pickatlas (http://fmri.wfubmc.edu/software/PickAtlas) toolbox, applying a dilation factor of 2. The MTL mask was also created using the WFU-Pickatlas. The MTL was defined as hippocampus, parahippocampus, and amygdala (Nolte 2009; Yang, Pan et al. 2012). Again a dilation factor of 2 was chosen.

Second, we assessed test-retest reliability of the paradigms using ICCs as described under 2.5.6. We used the ICC(3,1)-type (Shrout and Fleiss 1979) computed as ICC = $(\sigma^2_{between} - \sigma^2_{within}) / (\sigma^2_{between} + \sigma^2_{within})$. The variance components were calculated by the individual contrast values (i.e. con-images) separately for each session. According to established standards, reliability was classified as "poor" for ICC ≤ 0.40, as "fair" for $0.40 < ICC \leq 0.60$, as "good" for $0.60 < ICC \leq 0.80$, and as "excellent" for ICC > 0.80. ICCs were calculated using the matlab-based ICC toolbox provided by Caceres and colleagues (Caceres 2008). This toolbox calculates an ICC value for each voxel and allows referencing the reliability of brain activity (expressed by the ICC) to the strength of brain activity (expressed by the t-value). For specific regions of interest (ROI), the ICC can then be expressed as median value of the distribution of the ICC in the corresponding ROI.

As it turned out (see results section), the overall test-retest reliability of the paradigms was below the cutoff of 0.4 and has to be therefore classified as poor. One reason might be found in the calculation procedure of the ICCs. While ICC maps calculated on a voxel-by-voxel basis allow assessing the reliability of a paradigm for all brain regions,

this approach is also prone to random noise. In a second step, we therefore also calculated ICCs for predefined ROIs; that is, we first calculated some form of mean activation value (either by the mean value for all voxels in the ROI, the median value, or the maximum value within the ROI), then calculated the ICC. This procedure, also implemented in the ICC toolbox provided by Caceres and colleagues (Caceres 2008) is supposed to decrease the influence of random noise. ICCs were calculated for the left and for the right MTL. ROI masks created were created with the WFU-Pickatlas containing the left or right hippocampus, parahippocampus and amygdala (dilation factor 1). As reference reliability value, we also calculated ICC values for Broca area 44 (words paradigm) and for the fusiform gyrus (scenes paradigm, fractals paradigm). These structures were most active during the respective paradigms and were thus considered to potentially have the highest reliability values.

4. Results

In this chapter, I present the results of the conducted experiment; give examples of created imagery and tables of calculated LIs. First, I will present the group results calculated from the first measurement of all 20 subjects (4.1). Second, I will present the results of the reliability analysis (4.2).

4.1 Group Results

In the following chapter, I present the group results of the first measurement separately for each of the four paradigms (see 3.1). The overall activation level between the "New"- and the "Old"-condition strongly differed between the paradigms. I therefore chose different statistical thresholds to display the activation pattern, ranging from $p<0.01$ (uncorrected) to $p<0.00001$ (uncorrected). Lateralization indices were computed for each paradigm to describe the laterality of MTL brain activity. An index of >0.2 denotes left-lateralized activity, an index of <-0.2 right-lateralized activity. All indices between 0.2 and -0.2 were considered as bilateral.

4.1.1 Fractal Paradigm

At first, I present the whole brain activation patterns for the fractal paradigm, both as glass brain projection (Figure 17) and as 3D image (Figure 18). To exclude white matter artifacts a grey matter ROI mask (dilation factor 2), produced using the WFU Pickatlas, and was applied. I chose a cluster size (CS) threshold of 20 to eradicate small clusters.
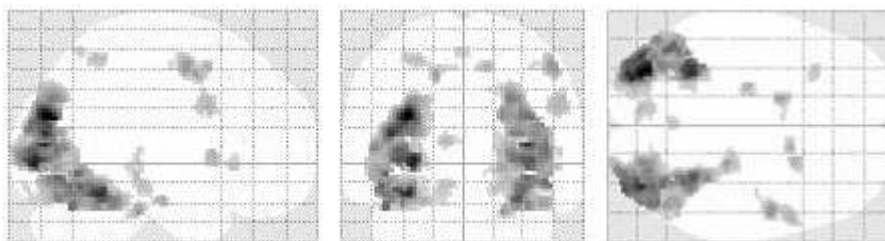
Figure 17: Activated brain regions associated with the encoding of fractals (first run, group analysis, contrast new > old, p<0.001 uncorrected, CS =20). Activated areas are shown as through-projections onto representations of MNI space
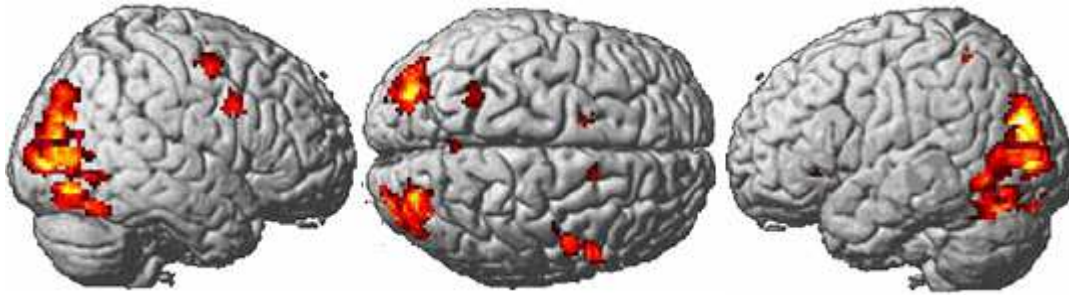
Figure 18 Activated brain regions associated with the encoding of fractals (first run, group analysis, contrast new > old, p<001 uncorrected, CS =20). Activations are rendered on the surface of the standard SPM8 template.

Main activation clusters were found in the visual cortex, the motor cortex areas, the bilateral MTL and the left frontal area. For an exact anatomical description of the activated clusters refer to the table below (Table 1). Interestingly the same motor-task produces a difference in activation in the new>old analysis. The higher general activation during a new task resulting in a top-down-modulation during the new task is a probable reason for this.

T-Value	Cluster size	X	Y	Z	Anatomical Location
10,15	1931	-32	-78	26	Left Middle Occipital Gyrus
8,60	2477	6	-80	10	HOC3-5, Area 17
5,61	95	2	-2	50	Area 6 (premotor cortex)
5,35	51	16	4	48	Area 6 (premotor cortex)
5,05	34	14	12	52	Right Superior Frontal Gyrus
4,95	24	-22	-14	-20	Left Hippocampus
4,77	30	2	14	4	Right Putamen
4,75	100	4	12	30	Right Inferior Frontal Gyrus, Area 44/45
4,71	110	24	-28	-8	Hippocampus (SUB)
4,70	37	10	-80	12	Left Calcarine Gyrus, Area 17/18
4,60	61	-28	-48	56	Left Inferior Parietal Lobule Area 2/ SPL
4,49	50	-8	-74	-12	Left Cerebellum
4,29	25	32	26	-2	Left Inferior Frontal Gyrus

4,22	20	2	-60	60	Left Precunius SPL

Table 1 Fractal paradigm
**Group analysis (ROI GM), CS=20, first run, p<0.001 uncorrected: For each anatomical location exemplary MNI coordinates and T scores are given. They refer to maximally activated foci as indicated by the highest T score within an anatomical region.**

In a second step, I specifically investigated brain activation in the MTL using a ROI mask including the hippocampus, parahippocampus and amygdala. The MTL brain activation is presented at p<0.001, uncorrected, both on a glass brain projection (Fig. 19) and on a coronal and sagittal slice (Fig. 20). Both the left and the right MTL is activated, but the right-sided activation is clearly stronger than the left.
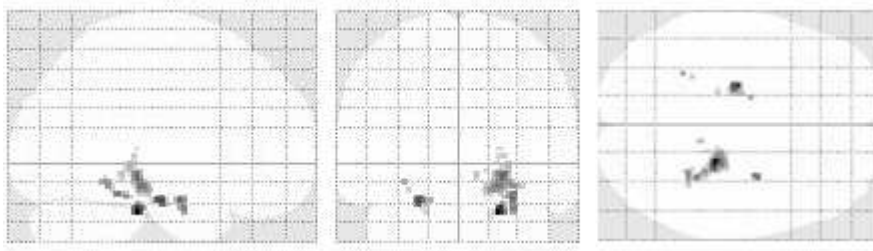
Figure 19 Fractal paradigm: Glass brain projection of the activation found at p<0.001 CS=0 uncorrected in the Group analysis (ROI MTL)
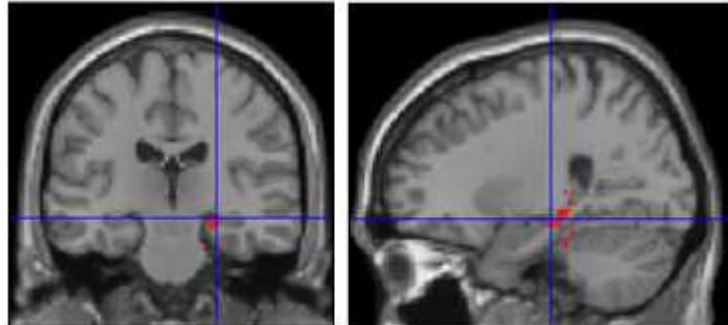
Figure 20 Fractal paradigm: Slice brain projection of the activation found at p<0.001 CS=0 uncorrected in the Group analysis Group analysis (ROI MTL)

To confirm this observation, lateralization indices were calculated for various statistical thresholds (Table 2). This analysis supports that overall there is a clear right-sided lateralization with LIs ranging from 0.22 to 0.59. As p-values get more conservative, the right lateralization is more distinctly expressed.

Fractals	Cluster size			
P-value	R	L	Lateralization	LI
0.001	96	26	R	-0.59
0.01	717	269	R	-0.45
0.05	1460	936	R	-0.22

Table 2 Fractal paradigm: Lateralization indices calculated for group analysis from right (R) and left (L) brain clusters using a ROI (HC, PHC, AM), CS=0 at p<0.001 uncorrected

4.1.2 Words Paradigm

At first, I present the whole brain activation patterns for the words paradigm, both as glass brain projection (Fig. 21) and as 3D image (Fig. 23). To exclude white matter artifacts, a grey matter ROI mask (dilation factor 2), produced using the WFU Pickatlas, was applied. I chose a cluster size (CS) threshold of 20 to eradicate small clusters.
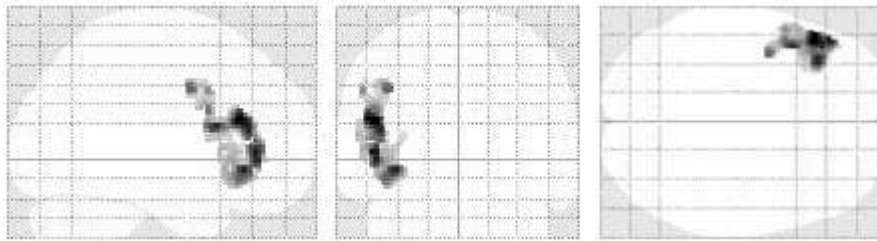
Figure 21 Words paradigm: Glassbrain projection of the activation found at p<0.001 CS=20 uncorrected in the Group analysis. A grey matter (GM) ROI was applied.

The table shows the anatomical allocation of the activated areas larger than 20 voxels. The main activation lies inside the Broca area (44/45)

T-Value	Cluster Size	MNI-Coordinates	Anatomical Correlate
5.55	509	-46 28 20	Left inferior Gyrus Area 44/45
5.14	276	-36 22 -6	Left inferior frontal Gyrus

Table 3 Words paradigm: Clusters and anatomical correlates found at p<0.001 uncorrected, with a CS=20 in the group analysis.

Due to the weak activation a more liberal approach was deemed necessary; therefore a threshold of p<0.01 (uncorrected) was applied.
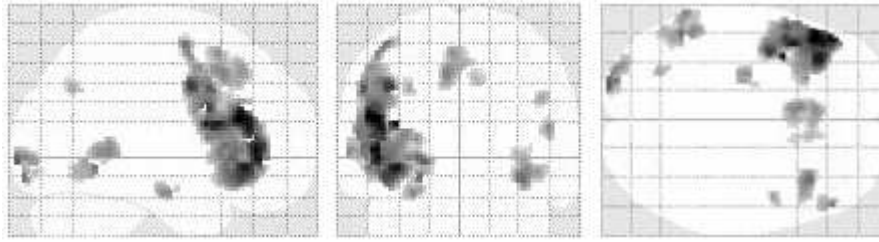
Figure 22 Words paradigm: Glass brain projection at p<0.01 uncorrected and CS=20 for group analysis.
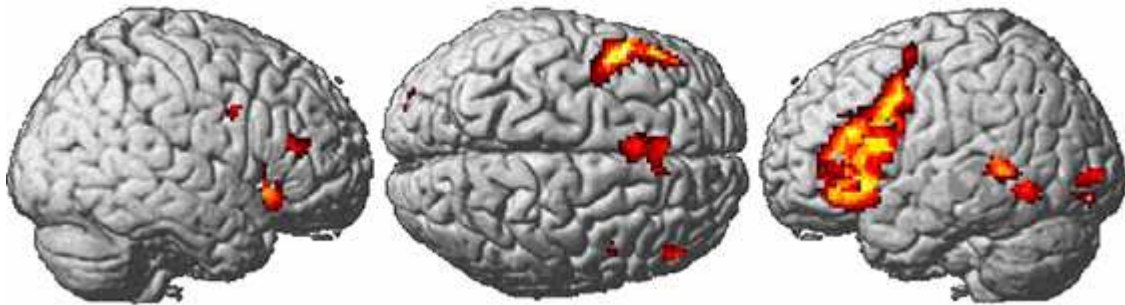
Figure 23 Words paradigm: Render plot of activated clusters at p<0.01 uncorrected CS=20, group analysis.

Main activation clusters were found in mostly the Broca area, smaller ones in the visual cortex, the motor cortex areas, the bilateral MTL and amygdale. For an exact anatomical description of the activated clusters refer to the table below (Table 3).

| Clustersize	MNI - Coordinates	Area
2608	-43 16 19	Left 44/45/6
350	-4 18 53	Left and right 6
234	37 20 -1	Right 45
175	-56 -51 10	Left middle temporal gyrus
127	-25 -95 3	Left hOC3v/hOC4v/17/18
116	-49 -62 -1	Left inferior temporal gyrus
70	-26 -18 -13	Left Hippocampus(CA)/left Amygala/left Hippocampus(FD)
48	49 32 20	Right 45
46	10 20 48	Right superior medial gyrus
31	-28 -69 43	Left HIP3/hIP1/IPC
27	46 1 37	Right 44

Table 4 Words paradigm: Activated anatomical areas at p<0.001 uncorrected CS=20

In a second step, I specifically investigated brain activation in the MTL using a ROI mask including the hippocampus, parahippocampus and amygdala. The MTL brain activation is presented at p<0.001, uncorrected, both on a glass brain projection (Fig. 24) and on a coronal and sagittal slice (Fig. 25). Both the left and the right MTL is activated, but the left-sided activation is clearly stronger than the right.
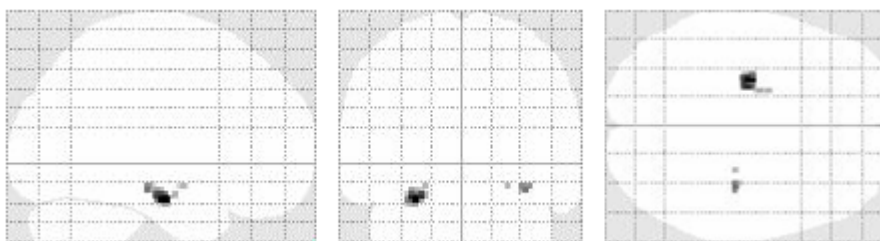
Figure 24 Words paradigm: Glass brain projection of the activation found at p<0.01 CS=0 uncorrected in the Group analysis using a ROI (MTL)
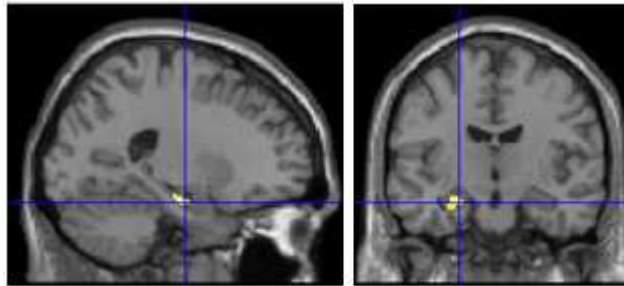
Figure 25 Words paradigm: Sliced Brain projection of the activation found at p<0.01 uncorrected CS=0 in the Group analysis using ROI (MTL)

To confirm this observation, lateralization indices were calculated for various statistical thresholds (Table 5). This analysis supports that, overall, there is a clear left-sided lateralization with LIs ranging from 0.56 to 1. As p-values get more conservative the left lateralization is more distinctly expressed.

Words	Clustersize		Lateralization	
P-value	R	L		LI
0.001	0	2	L	1
0.01	10	73	L	0.76
0.05	97	341	L	0.56

Table 5 Words paradigm: Lateralization indices calculated for group analysis from right (R) and left (L) using a ROI (MTL) and CS=0.

4.1.3 Scenes Paradigm

At first, I present the whole brain activation patterns for the scenes paradigm, both as glass brain projection (Fig. 26) and as 3D image (Fig 27). To exclude white matter artifacts a grey matter ROI mask (dilation factor 2), produced using the WFU Pickatlas, and was applied. I chose a cluster size (CS) threshold of 20 to eradicate small clusters.
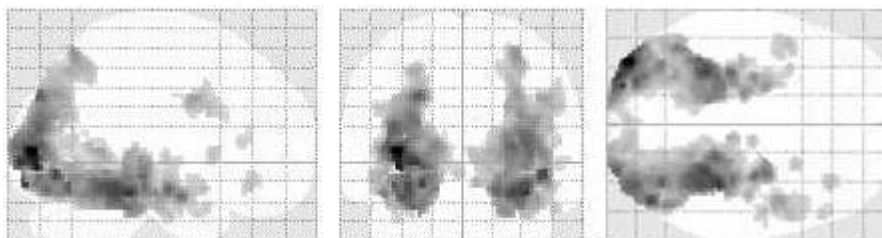
Figure 26 Scenes paradigm: Glass brain projection of activation found at p<0.001 uncorrected, ROI (GM), CS=20.
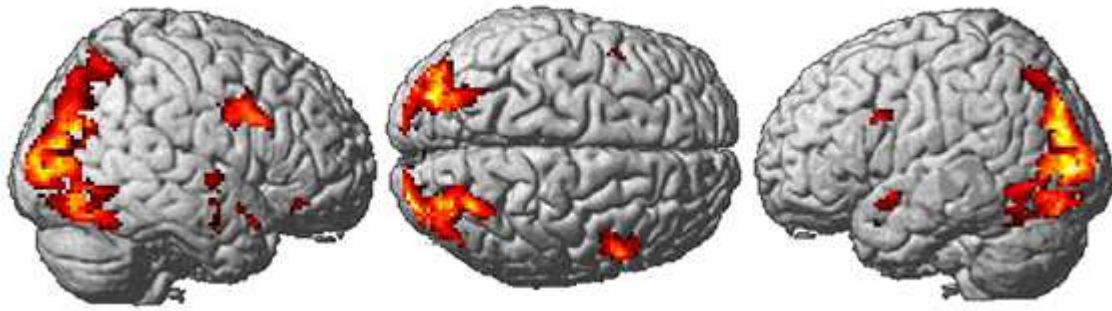
Figure 27 Scenes paradigm
Render of Group analysis (ROI GM), CS=20, first run, p<0.001 uncorrected

Main activation clusters were found in the visual cortex, the right MTL and the right frontal area. For an exact anatomical description of the activated clusters refer to the table below (Table 6). Interestingly the same motor-task produces a difference in activation in the new>old analysis. The higher general activation during a new task resulting in a top-down-modulation during the new task is a probable reason for this.

T-Value	Cluster size	MNI-Coordinates	Probable Anatomical Location
12,06	5147	-38 -88 6	Left Middle Occipital Gyrus Hippocampus (SUB)/(CA)/Area 17
9,65	5770	36 -32 -16	Right Fusiform Gyrus/ Hippocampus (CA)
5,82	395	44 4 34	Right Inferior Frontal Gyrus Area 44/45
8,03	39	10 -12 2	No Match
4,98	65	-46 10 -14	Left Temporal Pole
4,60	73	-44 12 28	Left Inferior Frontal Gyrus Area 44
4,59	25	50 -4 -14,	Right Middle Temporal Gyrus
4,55	29	24 14 4	Right Putamen
4,49	59	32 34 -14	Right Inferior Frontal Gyrus
4,38	37	54 -8 0	Right Superior Temporal Gyrus TE 1.2/1.0
4,27	32	42 14 -22	Right Temporal Pole

Table 6 Scenes paradigm: For each anatomical localization exemplary MNI coordinates and T scores are given. They refer to maximally activated foci as indicated by the highest T score within an anatomical region. CS=20, p<0.001 uncorrected;

In a second step, I specifically investigated brain activation in the MTL using a ROI mask including the hippocampus, parahippocampus and amygdala. The MTL brain activation is presented at p<0.001, uncorrected, both on a glass brain projection (Fig. 28) and on a coronal and sagittal slice (Fig. 29). Both the left and the right MTL are almost equally activated with a tendency to the right. I plotted activations at a more conservative threshold to differentiate the lateralization.

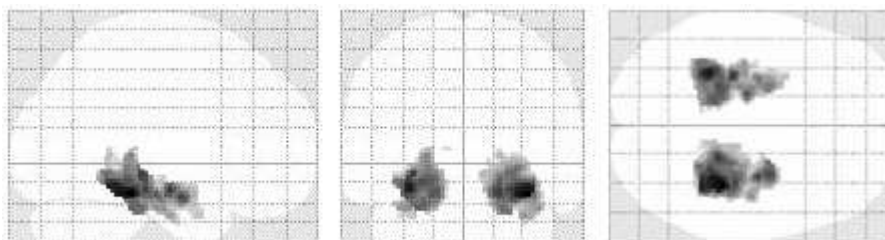**Figure 28 Scenes paradigm: Glass brain projection of activation found at p<0.001 uncorrected ROI (MTL), CS=0.**
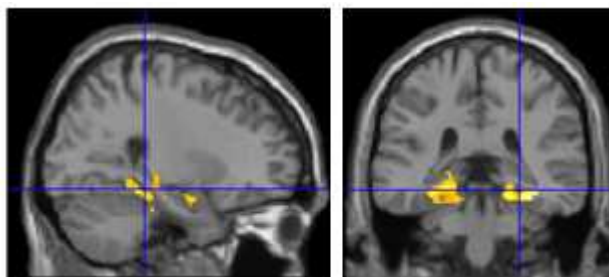
Figure 29 Scenes paradigm
Sliced image of results for group analysis ROI (MTL) CS=0, first run, p<0.00001 uncorrected
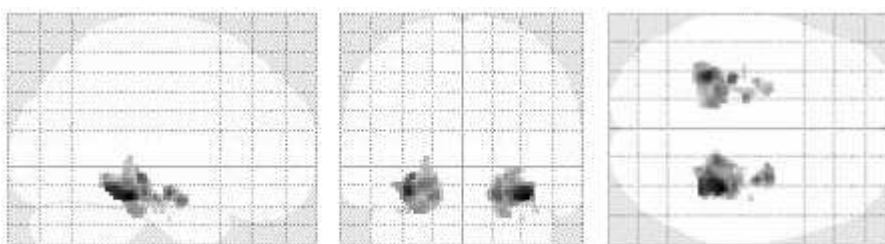
Figure 30 Scenes paradigm: Glass brain projection of activation found at p<0.05 FWE corrected, ROI (MTL), CS=0.
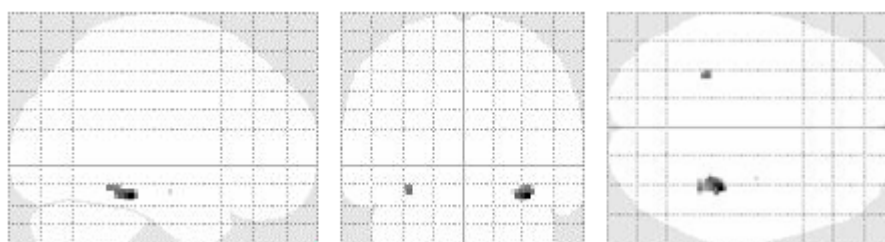
Figure 31 Scenes paradigm: Glass brain projection of activation found at p<0.000001 uncorrected ROI (MTL), CS=0.

To confirm this observation, lateralization indices were calculated for various statistical thresholds (Table 7). This analysis supports that, overall, there is a clear bilateral lateralization with LIs ranging from -0.01 to -0.07. As p-values get more conservative, the bilateral lateralization almost stays the same. However, it has to be stated that at the conservative correction of p<0.000001 the right-sided MTL activation is much stronger than the left.

Scenes	Clustersize			
P-value	R	L	Lateralization	LI
0.001	1676	1447	B	-0.07
0.01	2309	2113	B	-0.04
0.05	2640	2588	B	-0.01

Table 7 Indoor-Outdoor paradigm: Lateralization indices calculated for group analysis from right (R) and left (L) using a ROI (MTL), CS=0.

4.1.4 Faces Paradigm

At first, I present the whole brain activation patterns for the scenes paradigm, both as glass brain projection (Fig. 32) and as 3D image (Figure 33). To exclude white matter artifacts, a grey matter ROI mask (dilation factor 2), produced using the WFU Pickatlas, and was applied. I chose a cluster size (CS) threshold of 20 to eradicate small clusters.
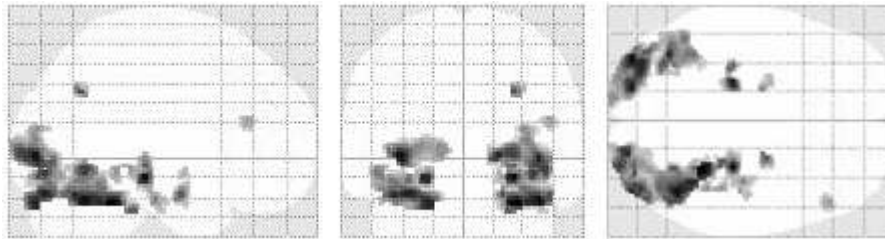
Figure 32 Faces paradigm: Glass brain projection of activation found at p<0.001 uncorrected ROI (GM), CS=20.

Figure 33 Faces paradigm
Render of group analysis activations at (ROI GM), CS=20, first run, p<0.001 uncorrected

Activated clusters are found in the hippocampus, the inferior occipital gyrus and also in the cerebellum and Broca's area. The overall level of activation is, at first sight, weaker than in the scenes paradigm. In the table below all activated clusters larger than 20 voxels are shown and their probable anatomical area is assigned.

T-Value	Clustersize	MNI-Coordinates	Probable Anatomical Location
6,42	1377	30 -44 -24	Right Cerebellum/Right Inferior Occipital Gyrus
6,18	173	28 -24 -10	Right Hippocampus (SUB)
6,09	342	-36 -86 2	Left Middle Occipital Gyrus hOC5
5,91	811	-30 -80 -20	Left Cerebellum
5,86	92	-22 -24 -10	Left Hippocampus (SUB)/(CA)
5,41	30	28 -60 36	hIP3
5,27	42	22 -4 -20	Right Parahippocampal Gyrus Hipp (EC)
4,80	52	36 -18 -22	Right Parahippocampal Gyrus Hipp (CA)
4,62	35	-18 -6 -20	Left Parahippocampal Gyrus Amygdale
4,35	43	48 34 20	Right Inferior Frontal Gyrus Area 45

Table 8 Faces paradigm
Activated clusters in group analysis (ROI GM), CS=20, first run, p<0.001 uncorrected

Again, visual areas are activated and on the right side hippocampal, as well as parahippocampal activation is recorded. The next pictures using the already introduced hippocampal ROI illustrate the MTL activation.
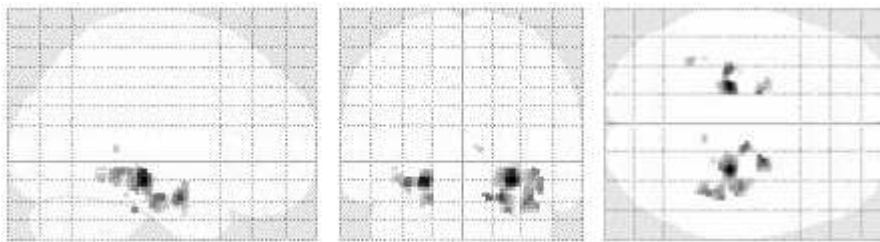
Figure 34 Faces paradigm: Glass brain projection of activation found at p<0.001 uncorrected ROI (MTL), CS=0.
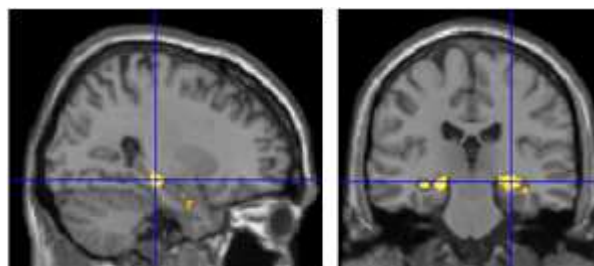
Figure 35 Faces paradigm
Sliced image activations at group analysis (ROI MTL), CS=0, first run, p<0.001 uncorrected

This image illustrates right accentuated hippocampus activation. Activations are found on both sides as expected. A more conservative correction was applied and the results showed a bilateral activation at p<0.05 FEW corrected.

Figure 36 Faces paradigm: Glass brain projection of activation found at p<0.05 (FWE corrected) ROI (MTL), CS=0.

As done for the other paradigms LIs were calculated for operational purposes. The resulting LIs ranged from 0.18 to 0.41 painting an ambiguous image. At p<0.05 (uncorrected) lateralization is bilateral, but at 0.01 and 0.001 it results right lateralized.
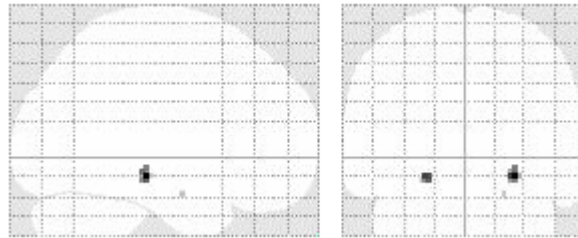
Faces	Clustersize		Lateralization	
P-value	R	L		LI
0.001	321	133	R	-0.414
0.01	1309	620	R	-0.357
0.05	2199	1532	B	-0.179

Table 9 Faces paradigm Lateralization indices calculated for group analysis from right (R) and left (L) using a Group analysis (ROI MTL), CS=0.

4.2 Reliability

The reliability of brain activation was assessed by ICCs (see chapter 3.3.1). In a first step, ICC maps were calculated voxel-by-voxel separately for each paradigm[1] (4.2.1). In a second step, ICCs were calculated for predefined ROIs (4.2.2).

4.2.1 ICC maps calculated for each voxel

First, the ICC maps will be characterized by a median ICC for the whole brain, for the activated network and for the deactivated network. Graphically, I also depict the ICC maps by showing the relative voxel frequency of ICC values as a histogram. Second, the relationship between the ICC values and the corresponding t-values is analyzed to investigate whether, in general, brain regions with stronger activation or deactivation

---

[1] I did not measure the subjects a second time using the faces paradigm. Therefore I calculated reliability values only for three paradigms.

also show higher reliability. Third, I present the overlapping brain activation pattern of the first and the second measurement in a 3D image.

Fractals paradigm

Median ICCs for the whole brain, for the activated network and for the deactivated network are presented in Table 10. Overall, the reliability must be characterized as poor (all median ICCs < 40). Even for the activated network, defined by those voxel that were activated at p<0.01 uncorrected, the median ICC is only ~12. A frequency distribution for the ICCs in the whole brain, in the activated and in the deactivated network is plotted in Figure 37

Category	Median ICC (x100)
Brain	-8.51
Network	11.95
Deactivated Network	0.57

Table 10 1Fractals paradigm, t=3.79, p=0.01(uncorrected), Cluster size=10: Reliability of the fractals paradigm was assessed by whole brain ICC maps. Median ICC values for the whole brain, the activated network and the deactivated network are presented.
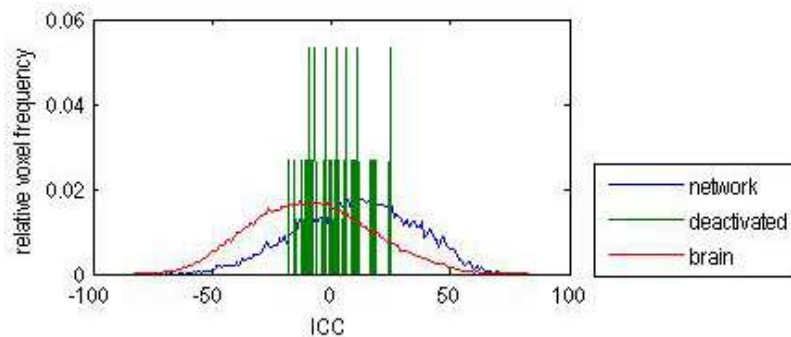
Figure 37 Fractals paradigm, t=3.79, p=0.01(uncorrected): The figure shows a plot of the relative voxel frequency over the ICC for all voxels in the brain, the activated and the deactivated network (based on the first run).

Whole brain joint probability distributions showed an association between t-values and ICCs in the sense that ICCs were generally higher within brain regions showing high brain activity (Figure 38). The ICC cloud is slightly V-shaped and the apex is just between 0 and 2. Almost all points lie between -50 and 50 on the y-axis representing the ICC values. As the t-score rises, the ICCs also increases, but even single voxels in this distribution never reach a level of above 60, marking the threshold to high significance.
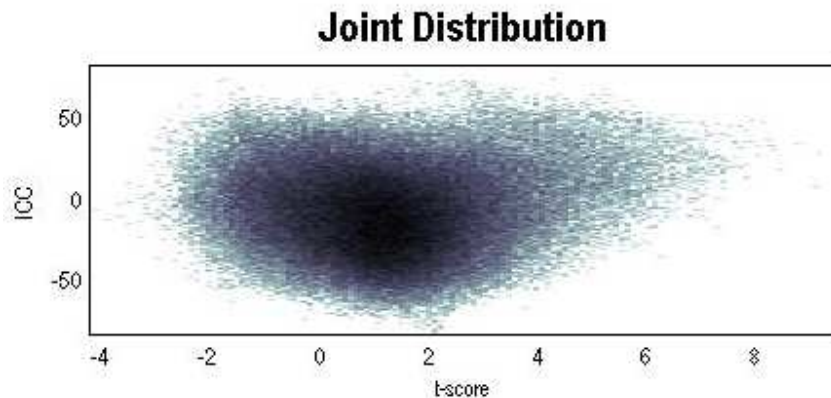
Figure 38 Fractals paradigm, t=3.79, p=0.01(uncorrected): Joint distribution of according voxel-wise t-scores (first run) and associated ICCs.

Brain activity for both the first and the second measurement is depicted by in figure 39. One can clearly see that the extent of brain activation is much higher for the first than for the second run. Although the same network is active in both runs (as can be seen when less stringent statistical thresholds are applied for the second measurement), the strength of brain activation, that is the contrast between both conditions, is lower in the second run. This explains the low ICCs for the fractals paradigm.
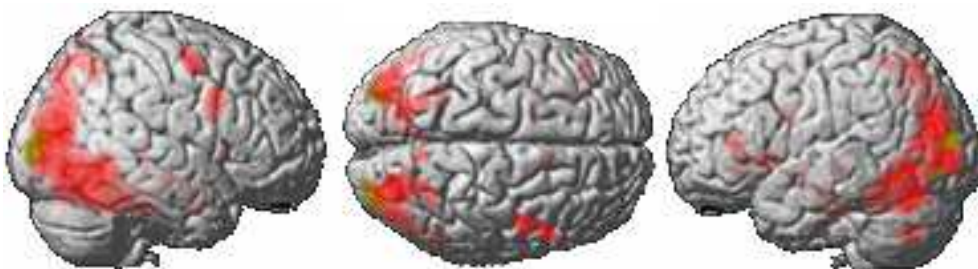
Figure 39 Brain activation overlay for fractals paradigm (group results, contrast new>old, p<0.01 uncorrected, CS = 10) for the first (red) and the second (green) measurement.

Scenes paradigm

Median ICCs for the whole brain, for the activated network and for the deactivated network are presented in Table 11. Overall, the reliability must be characterized as poor (all median ICCs < 40). Even for the activated network, defined by those voxel that were activated at p<0.01 uncorrected, the median ICC is better than the one resulting

from the fractals paradigm, at ~34. A frequency distribution for the ICCs in the whole brain (red), in the activated (blue) and in the deactivated (green) network is plotted in figure 40.

Category	ICC (x100)
Brain	14.4
Network	34.66
Inactivated Network	31.69

Table 11 1st run t-test Scenes paradigm, t=3.79, p=0.01, Cluster size =10: Reliability of the scenes paradigm was assessed by whole brain ICC maps. Median ICC values for the whole brain, the activated network and the deactivated network are presented.


Figure 40 1st run t-test Scenes paradigm, t=3.79, p=0.01, Cluster size =10: The figure shows a plot of the relative voxel frequency over the ICC for each network, deactivated and whole brain analysis.

The joint distribution plot stretches further out to the higher t-values and the slightly higher ICCs. The higher ICCs can also be seen in the graph of the relative voxel frequency over ICCs, where the apex of the curve is moved to the right compared to the one of the words paradigm. This reflects the higher ICCs calculated for this paradigm.
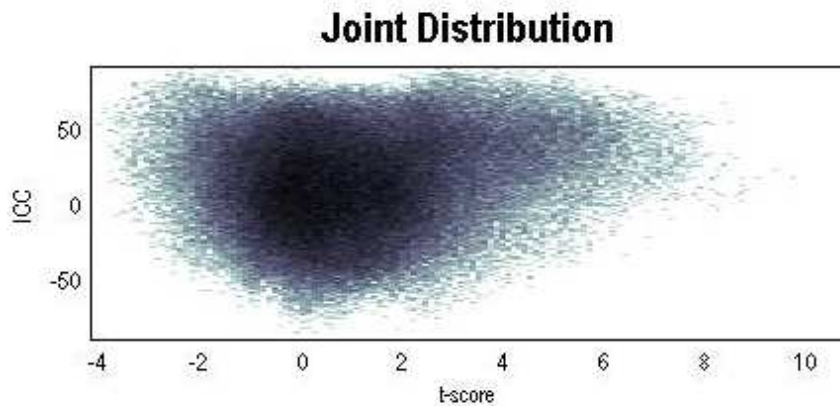
Figure 41 1st run t-test Scenes paradigm, t=3.79, p=0.01, Cluster size =10: Joint distribution (first run) of according voxel-wise t-scores and associated ICCs.

Brain activity for both the first (red) and the second (green) measurement is depicted by in figure 42. One can clearly see that the extent of brain activation is higher for the first than for the second run. Although the same network is active in both runs (as can be seen when less stringent statistical thresholds are applied for the second measurement), the strength of brain activation, that is the contrast between both conditions, is lower in the second run (green). This explains the low ICCs for the scenes paradigm.
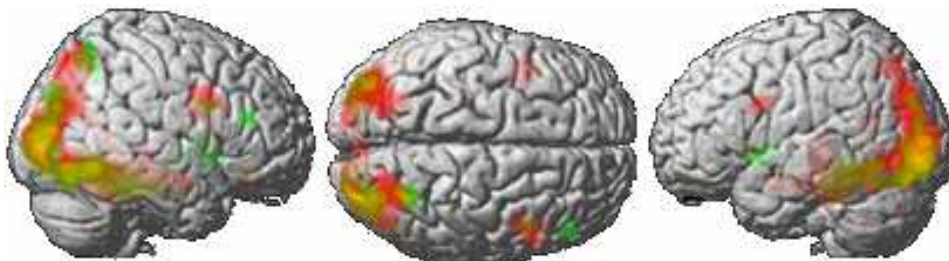
Figure 42 Brain activation overlay for scenes paradigm (group results, contrast new>old, p<0.01 uncorrected, CS = 10) for the first (red) and the second (green) measurement.
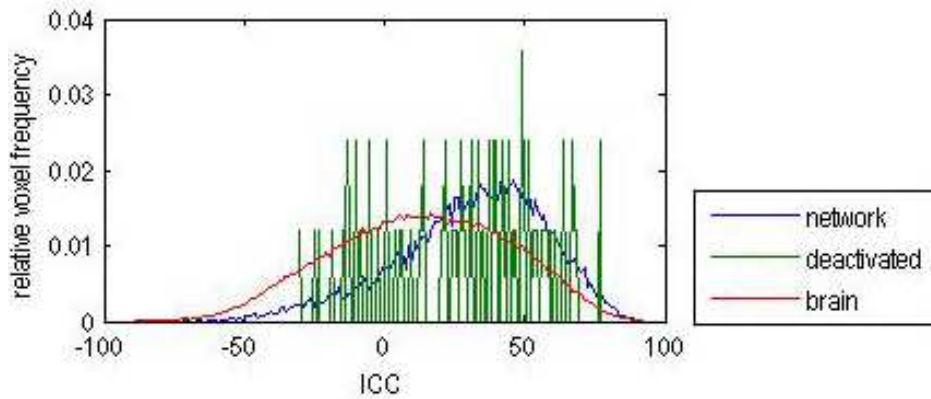
Words paradigm

Median ICCs for the whole brain, for the activated network and for the deactivated network are presented in Table 12. Overall, the reliability must be characterized as poor, similar to the fractals paradigm (all median ICCs < 40). Even for the activated network, defined by those voxel that were activated at p<0.01 uncorrected, the median ICC is only ~15. A frequency distribution for the ICCs in the whole brain (red), in the activated (blue) and in the deactivated (green) network is plotted in Figure 43

47

Category	ICC (x100)
Brain	16.9
Network	14.91
Deactivated Network	15.95

Table 12 1st run t-test Words paradigm, t=2.6, p=0.01, Clustersize=10: Reliability of the words paradigm was assessed by whole brain ICC maps. Median ICC values for the whole brain, the activated network and the deactivated network are presented.
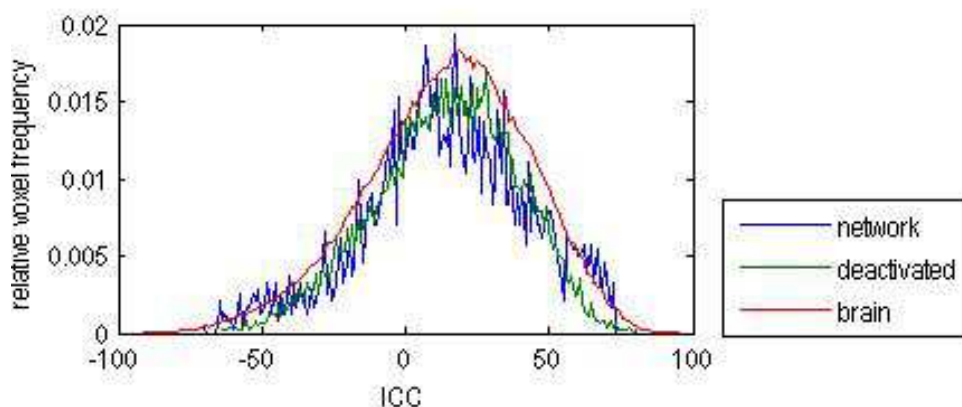

Figure 43 1st run t-test Words paradigm, t=2.6, p=0.01, Clustersize=10): The figure shows a plot of the relative voxel frequency over the ICC for each network, deactivated and whole brain analysis.

It is notable that the resulting curves in Fig. 46 undulate much less than those seen for the scenes and fractals paradigms.

The plot for the joint distribution (Fig 48) shows a more circular shaped picture with a tail reaching towards the negative t-score regions. Its apex lies just below 0 on the x-axis.
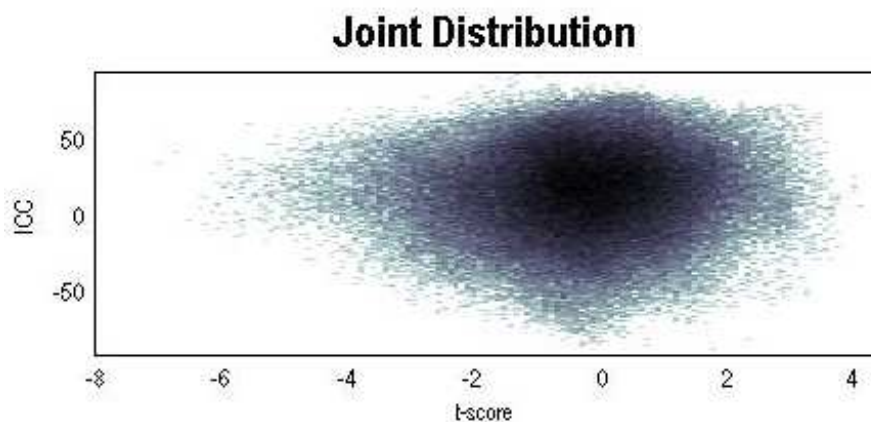
Figure 44 1st run t-test Words paradigm, t=2.6, p=0.01, Clustersize=10 Joint distribution of according voxel-wise t-scores and associated ICCs.

Brain activity for both the first (red) and the second (green) measurement is depicted by in figure 45. One can clearly see that the extent of brain activation is almost equal for the first than for the second run. Although roughly the same network is active in both runs (as can be seen when less stringent statistical thresholds are applied for the second measurement), the strength of brain activation, that is the contrast between both conditions, is lower in the second run (green) and the general overlap is not given for all clusters at this threshold. This explains the low ICCs for the words paradigm.
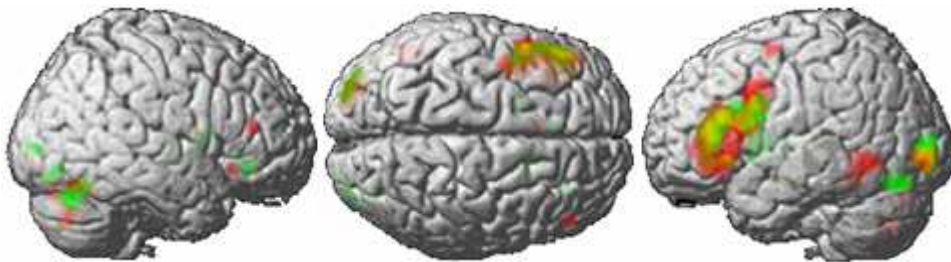
Figure 45 Brain activation for words paradigm (group results, contrast new>old, p<0.01 uncorrected, CS = 10) for the first (red) and the second (green) measurement.

### 4.2.2 ICCs for predefined ROIs

The overall test-retest reliability of all paradigms was below of 40 and has to be therefore classified as poor. One reason might be that ICC maps, which are calculated voxel-by-voxel, are relatively prone to random noise. I therefore also calculated ICCs for predefined ROIs (see 3.3.1). For all paradigms, ROI-based ICCs were, on the one hand, calculated for the left and for the right MTL, on the other hand, for a reference ROI. As reference ROI, I chose the cluster of highest activation. With regard to the fractals paradigm the activated cluster in the left and right fusiform gyrus were chosen, extracted from the resulting data and used as reference ROI1 and reference ROI2 for the ICC calculation. This process was accordingly done with the same result for the scenes paradigm. The words paradigm did not show a large activation in the fusiform gyrus, therefore the highly-activated Broca region was chosen as reference ROI1. Only one reference ROI was chose because of the unilateral nature of the Broca region.

For each ROI, three different activation values were extracted, either using the mean activation of all voxels in the ROI, the median activation or the maximum activation value. The resulting ICC values for each paradigm are listed in Table 19.

The fractals paradigm produced negative ICCs for all three ROIs, showing very low overall reliability. Also the reliability for the words paradigm was low, even with regard to the brain activity in the Boca's region. In line with the results from the ICC maps, the reliability of the scenes paradigm was the highest, but overall also on a relatively low level. Only brain activity in the left fusiform gyrus yielded relatively stable ICC with a value of ~0.43.

The fractals paradigm produced negative ICCs for all three ROIs. The results can be seen in the following table 13.

ROIs /Calculation Method	ROI-ICC Fractals (x100)	ROI-ICC Scenes (x100)	ROI-ICC Words (x100)
MTL_li			
Max	-6.64	19.14	-04.73
Mean	-53.72	-7.74	1.06
Median	-53.78	19.11	-3.57
MTL_re			
Max	-14.7	2.52	-13.6
Mean	-55.56	3.81	30.93
Median	-55.82	3.28	28.8
reference ROI1			
Max	2.7	32.97	-16.44
Mean	-13.28	42.49	-7.68
Median	-10.99	44.65	
reference ROI2			
Max	29.07	74.95	
Mean	-9.68	28.32	
Median	-9.83	28.2	

Table 13 ICCs calculated for each paradigm. Reference ROI1 reefers to left fusiform gyrus for scenes and fractals paradigms and to Broca area 44/45 for words paradigm. Reference ROI2 refers to right fusiform gyrus.

The scenes paradigm showed higher ICCs for all different ROIs. Both left and right MTL ROIs stayed below the 0.4 cutoff for weak significance, the right coming close with ~0.38 for the mean ICC. The left fusiform ROI produced weak significant results, stating a mean ICC of ~0.42 and a median ICC of ~0.45. The strongest results were observed for the max ICC of the reference ROI2 with a strong ICC of ~0.75, while max and mean ICCs stayed below the 0.4 cutoff. Table 19 shows the exact results.

Looking at the words paradigm, generally weak results are observed. The left MTL ROI and the Broca ROI show now ICC correlation. Only the mean ICC of the MTL shows a very week correlation of 0.31. All ICC results are displayed in table 19.

5. Discussion

The present study had four objectives: the implementation of a memory encoding task at the new 3T MR-scanner in Marburg, the creation of two new stimulus classes for the paradigm, the improvement of non-verbalizeable stimulus material, and the analysis of the test-retest reliability of brain activity. In the following, I will discuss these four objectives in more detail.

5.1 Implementation of the paradigm

In the present study, I intended to develop and test a memory encoding paradigm that can be applied to investigate the neural correlates of memory processes, in particular within the medial temporal lobe, using fMRI. The main idea of the paradigm was to compare brain activity elicited by "new" stimuli, that is, stimuli that were shown only once during the experiment, and "old" stimuli, that is, stimuli that had been repeatedly shown before the measurements. I used four versions of this paradigm differing in the presented stimulus material: words, fractals, faces, scenes. A prototype of this paradigm had been already used in our research group in previous measurements at another MR-scanner. The first objective of this study was, therefore, to implement this paradigm at the new 3T MR-scanner in Marburg. Twenty healthy subjects were measured with each version of the paradigm. Brain activity was assessed on the group level for the contrast "new > old". A successful implementation of the paradigm would be achieved on the one hand by "meaningful" whole brain activation pattern, on the other hand by detectable brain activity within the MTL.

The implementation of the paradigm at the new 3T MR-scanner at the Philipps-University Marburg was successful. After only a small number of test runs, the system was set up and the actual data collection could commence. For visual stimulation, both video goggles and a LCD TV in combination with a mirror mounted directly over the subjects head were successfully used. Video goggles were used in particular for subjects with vision impairments because the goggles included an optic device capable of compensating these viewing impairments. For all subjects with good eye vision, visual stimuli were shown via TV screen since this method is easier to apply. A data analysis algorithm was established at the scanning facilities, so that future studies will be much easier to conduct. For all four stimulus classes, the whole brain activation pattern was

"meaningful"; that is, we detected, for instance, brain activity in Broca's area for the word encoding task or in the visual cortex for the fractal encoding task, in accordance with the results of previous memory encoding studies (Golby, Poldrack et al. 2001; Jansen, Sehlmeyer et al. 2009). In particular, we detected brain activity in the MTL for all four version of the paradigm.

A potential drawback of the paradigm might be that the brain activation differences between both conditions were relatively low. At the whole brain level, we had to apply non-corrected significance thresholds, in accordance with previous studies (Jansen, Sehlmeyer et al. 2009). In this context, the scenes paradigm performed best showing strong activated differences at an uncorrected significance threshold of p<0.001 (see Fig. 29). Especially well performed the ROI analysis. It produced significant hippocampal activation differences even at very conservative significance thresholds of p<0.000001 uncorrected (see Fig. 34) or p<0.05 FWE corrected (see Fig. 33). Second strongest performing paradigm was the faces paradigm, having strong activation differences at whole brain analysis (see Fig. 35) and also producing significant hippocampal activation differences at a significance threshold of p<0.05 FWE corrected in ROI analysis. Performing a little less strong at whole brain analysis using a significance threshold of p<0.001 was the fractals paradigm (see Fig. 20) whilst activation in ROI analysis was still recorded at p<0.001 during ROI analysis (see Fig. 23). The words encoding paradigm produced the weakest activation differences. Therefore, an uncorrected significance threshold of p=0.01 had to be applied to detect activation differences in other brain areas than Broca's area. Hippocampal activation was found during ROI analysis only at a significance threshold of p<0.01 (see Fig. 25). A possible reason might be that the "new" words had been known already by the subjects before, while for instance "new" fractals or new scenes were presented the first time in their life. Future studies will have to improve the overall sensitivity oft the paradigm, for instance, by using MR sequences specifically tailored to measure brain activity of the MTL. Summarizing I conclude a successful implementation of the existing paradigm at the research facilities in Marburg.

5.2 Creation of two new stimulus classes

The lateralization of brain activity during memory encoding depends on the type of stimulus material. Verbal stimuli allegedly activate preferentially left hemispheric

regions and non-verbal stimuli right hemispheric regions (Golby, Poldrack et al. 2001; Jansen, Sehlmeyer et al. 2009). The previous prototype of the paradigm only used two stimulus classes, words and fractals. In the present study I therefore intended to create two new stimulus classes with medium verbalizeable characteristics. These stimuli were supposed to elicit bilateral brain activity, in particular within the MTL.

I decided to choose, on the one hand, faces, on the other hand indoor- and outdoor scenes. I took the images for the faces paradigm from Minear et al. (Minear and Park 2004), resized them and implicated a task to differentiate between male and female faces was. The stimuli for the scenes paradigm I gathered from private and internet sources resized and attached the task of differentiating "indoor" from "outdoor" scenes. Both stimuli classes performed better than the original two classes, producing hippocampal FWE corrected activation differences in ROI analysis (see Results 4.1.3 and 4.1.4). The scenes paradigm showed bilateral activation at conservative threshold. Due to reasons of simplicity and time-effectiveness, which are important points regarding clinical implementation, I chose only the scenes paradigm, as the one showing good bilateral activation differences, to go into the reliability test alongside the two original stimulus classes. To summarize this, I can conclude a successful implementation of these new stimulus classes.

5.3 Development of stimuli with less verbalizeable patterns

My goal was to improve the performance of the hard to verbalize stimuli. I used abstract fractals as stimuli material and created them using specific software called Apophysis. The findings on group level in the results section show a strong right MTL activation difference (see 4.1.1) which indicates visual processing of the material according to Golby et al. (Golby, Poldrack et al. 2001). To operationalize the lateralization I calculated LIs in group analysis. The results showed right-sided activation ranging from -0.22 to -0.59 for the first measurement and -1 throughout the second measurement. Even though the findings differ substantially between measurements, they show a consistent right-sided MTL activation difference. This indicates that the fractals used in this study are less verbalizeable than the patterns used in earlier studies and are therefore are more suitable to activate the right-sided MTL. The different levels of right side activation may result from habituation effects, because the subjects were already

familiar with the task at hand during the second measurement. This resulted in lower overall activation but at the same time the right-sided activation became more imminent. To rule out effects of repetitive examination of the subjects, it would be necessary to let more time pass between the two measurement points. In this study, an average of 35 days lay between some subject's first and second measurement. As stated before, this may have lead to habituation effects lowering the overall cognitive level of excitation in the subjects. Furthermore, the long scanning times of approximately one hour for all four paradigms combined may have contributed to this effect. Future studies may address this by creating a higher level of cognitive activation through either offering bonuses for good results or increasing the pace of the paradigm and the connected choice task. To summarize this, I can conclude the successful implementation of less verbalizeable stimuli in comparison to the preliminary studies.

5.4 Testing reliability

My goal was to test reliability using ICC maps for individual results. Many authors published on memory encoding and hippocampal activity (Golby, Poldrack et al. 2001; Golby, Poldrack et al. 2002; Powell, Koepp et al. 2004; Deblaere, Backes et al. 2005; Narayan, Kimberg et al. 2005; Powell, Koepp et al. 2005; Avila, Barros-Loscertales et al. 2006; Branco, Suarez et al. 2006; Frings, Wagner et al. 2006; Haut and Barch 2006; Jansen, Sehlmeyer et al. 2009; Rosazza, Minati et al. 2009; Strandberg, Elfgren et al. 2011), but only few have addressed reliability in their respective studies (Machielsen, Rombouts et al. 2000; Wagner, Frings et al. 2005; Harrington, Tomaszewski Farias et al. 2006; Clement and Belleville 2009; Putcha, O'Keefe et al. 2011). Results have been very inhomogeneous since many different approaches to testing reliabilities have been taken. Looking at the overlook of published literature given by Bennett et al. (Bennett and Miller 2010) ICC maps and overlapping of clusters were the methods most commonly used. They also observed the following phenomenon: "Motor and sensory tasks seem to have greater reliability than tasks involving higher cognition" (Bennett and Miller 2010). This can be shown, for example in the Bosnell et al study (Bosnell, Wegner et al. 2008) which resulted in an ICC of 0.82. Tasks of higher complexity received generally lower ICC results (Harrington, Tomaszewski Farias et al. 2006; Caceres, Hall et al. 2009). This brings us to my paradigms classified as complex ones. The best performing scenes paradigm resulted at an ICC of roughly 75 in ROI analysis.

This is the only paradigm resulting in a significant ICC above 60. All other results were even below the weak reliability cutoff at 40. The afterwards implemented ROI-ICC also didn't show any significant results for the largest cluster for the fractals or words paradigm. Concluding, of all three paradigms only the ROI analysis (right fusiform gyrus) of the scenes paradigm showed significant reliability as far as ICCs are concerned.

Remembering that intra-class correlations compare the inter-subject variability to the intra-subjects variability, the results can be interpreted either as a lack of inter-subject variability or a high intra-subjects variability over the course of the two runs. Judging from the general results of this study, the most probable explanation is the latter. Looking at the individual results, the inter-subject variability is high. Also the intra-subject variability between the two runs of the study is quite high when one looks into the second level or first level results. This results in the too high intra-subject variability being the most probable explanations for the results shown in this study.

In future studies, this must be the benchmark of any reliability research. Throughout the literature, ICC analysis has not been used very often in fMRI studies (Bennett and Miller 2010), which can be seen as a weakness and results in a lack of credibility for fMRI as a scientific method. Using ICC analysis as a tool of thoroughly judging reliability might strengthen the stance of fMRI in the science world and may result in a better introduction into the clinical context.

6 Conclusion and Outlook

To draw a conclusion of this study, the following has to be taken into account. I could only, on levels of low significance, show the expected activations for some individual subjects and the group analysis. These results resemble those reported by Golby and colleagues (Golby, Poldrack et al. 2001) and those found by Sehlmeyer and colleagues (Jansen, Sehlmeyer et al. 2009) in the way that activations were only found at quite low significance levels (ranging from $p<0.01$ to $p<0.0001$ uncorrected). Still I do not draw the same conclusions. Golby and colleagues wrote: "Paradigms similar to that used in the present study may allow preoperative assessment of the competence of each MTL in supporting material-specific memory processes. Specifically, the present study suggests that the encoding of patterns, relative to faces or scenes, may offer a more selective method for identifying neural systems mediating non-verbal memory. Such knowledge could aid in localizing eloquent brain areas, predicting the laterality of seizure focus and preventing postoperative deficits" (Golby, Poldrack et al. 2001).

Taking into account the further knowledge of reliability, or the lack thereof, gained in this study, paradigms similar to the ones used here are a long distance away from clinical implementation in preoperative diagnostics. In opposition to what Golby and colleagues suggest, much work has to be put into the further refinement of the paradigms, to enhance the results to the significant and reliable level needed for clinical implementation. Similar to what was found in the Golby study, only the LIs are fairly consistent over the two points of measurement in second level analysis. But this isn't sufficient to introduce a similar paradigm into clinical use. To achieve this, consistent results on individual and group level would have to be proven. Therefore I see this paradigm as a promising vehicle of exploration of memory asymmetry, which needs to be enhanced to higher levels of significance on both first and second level analysis; furthermore, reliability has to be improved.

As an outlook, I display exemplary promising first level results of one subject. The subject shows the expected left-sided activation in the first run produced by the words paradigm at $p<0.01$ (uncorrected) (see Fig 46). Also the second run produces left-sided but considerably lower activation. See figure 47, where second run results are plotted in green over the red first run results. A much smaller activated cluster represents the second run, which has some overlapping regions with the first run. These results show

that certain areas can be reproduced in a rerun of the experiment. The much lower activation level in the second run could be explained by habituation effects. In the future, an experiment including two points of measurement where a higher degree of overlapping of information is registered, could lead to reliable results.
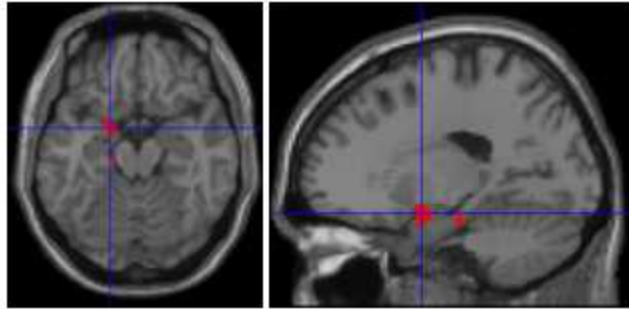
Figure 46 Sliced bran image of activation in words paradigm on single subject level.
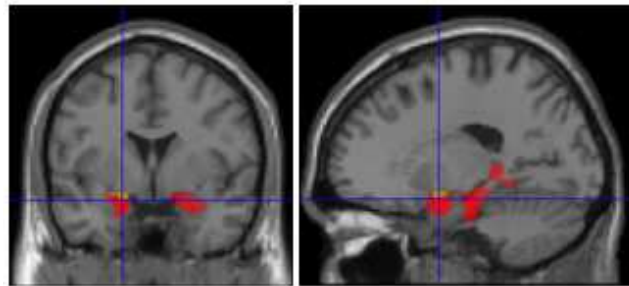
Figure 47 Sliced brain image containing first measurement activation (red) and second measurement activation (green) on single subject analysis for the words paradigm.

In my opinion, future studies will have to be measured, especially in the crucial point of reliability, to ensure moving fMRI memory lateralization closer to clinical use.

Literature

Akanuma, N., M. Koutroumanidis, et al. (2003). "Presurgical assessment of memory-related brain structures: the Wada test and functional neuroimaging." Seizure **12**(6): 346-58.

Atri, A., J. L. O'Brien, et al. (2011). "Test-retest reliability of memory task functional magnetic resonance imaging in Alzheimer disease clinical trials." Arch Neurol **68**(5): 599-606.

Avila, C., A. Barros-Loscertales, et al. (2006). "Memory lateralization with 2 functional MR imaging tasks in patients with lesions in the temporal lobe." AJNR Am J Neuroradiol **27**(3): 498-503.

Bennett, C. M. and M. B. Miller "How reliable are the results from functional magnetic resonance imaging?" Ann N Y Acad Sci **1191**: 133-55.

Bennett, C. M. and M. B. Miller (2010). "How reliable are the results from functional magnetic resonance imaging?" Ann N Y Acad Sci **1191**: 133-55.

Bosnell, R., C. Wegner, et al. (2008). "Reproducibility of fMRI in the clinical setting: implications for trial designs." Neuroimage **42**(2): 603-10.

Branco, D. M., R. O. Suarez, et al. (2006). "Functional MRI of memory in the hippocampus: Laterality indices may be more meaningful if calculated from whole voxel distributions." Neuroimage **32**(2): 592-602.

Caceres, A. (2008). ICC toolbox for SPM5. London, Centre for Neuroimaging Sciences Institute of Psychiatry
King's College London.

Caceres, A., D. L. Hall, et al. (2009). "Measuring fMRI reliability with the intra-class correlation coefficient." Neuroimage **45**(3): 758-68.

Clement, F. and S. Belleville (2009). "Test-retest reliability of fMRI verbal episodic memory paradigms in healthy older adults and in persons with mild cognitive impairment." Hum Brain Mapp **30**(12): 4033-47.

Deblaere, K., W. H. Backes, et al. (2005). "Lateralized anterior mesiotemporal lobe activation: semirandom functional MR imaging encoding paradigm in patients with temporal lobe epilepsy--initial experience." Radiology **236**(3): 996-1003.

Deetjen, P., E. J. Speckmann, et al. (2005). Physiologie, Urban & Fischer.

Eichenbaum, H. (2000). "A cortical-hippocampal system for declarative memory." Nat Rev Neurosci **1**(1): 41-50.

Engel, J., Jr. (1993). "Update on surgical treatment of the epilepsies. Summary of the Second International Palm Desert Conference on the Surgical Treatment of the Epilepsies (1992)." Neurology **43**(8): 1612-7.

Engel, J., Jr. (1996). "Surgery for seizures." N Engl J Med **334**(10): 647-52.

Freyer, T., G. Valerius, et al. (2009). "Test-retest reliability of event-related functional MRI in a probabilistic reversal learning task." Psychiatry Res **174**(1): 40-6.

Frings, L., K. Wagner, et al. (2006). "Gender-related differences in lateralization of hippocampal activation and cognitive strategy." Neuroreport **17**(4): 417-21.

Friston, K. J., Holmes, A.P. (1995c). "Statistical Parametric Maps in Functional Imaging:
A General Linear Approach." Human Brain Mapping **2**: 189-210.

Gabrieli, J. D. (1998). "Cognitive neuroscience of human memory." Annu Rev Psychol **49**: 87-115.

Golby, A. J., R. A. Poldrack, et al. (2001). "Material-specific lateralization in the medial temporal lobe and prefrontal cortex during memory encoding." <u>Brain</u> **124**(Pt 9): 1841-54.

Golby, A. J., R. A. Poldrack, et al. (2002). "Memory lateralization in medial temporal lobe epilepsy assessed by functional MRI." <u>Epilepsia</u> **43**(8): 855-63.

Harrington, G. S., S. Tomaszewski Farias, et al. (2006). "The intersubject and intrasubject reproducibility of FMRI activation during three encoding tasks: implications for clinical applications." <u>Neuroradiology</u> **48**(7): 495-505.

Haut, K. M. and D. M. Barch (2006). "Sex influences on material-sensitive functional lateralization in working and episodic memory: men and women are not all that different." <u>Neuroimage</u> **32**(1): 411-22.

Heeger, D. J. and D. Ress (2002). "What does fMRI tell us about neuronal activity?" <u>Nat Rev Neurosci</u> **3**(2): 142-51.

Jansen, A. (2004). Atypische Lateralisation Cognitiver Hirnfunktionen -Funktionelle MRT Topographie. <u>Humanmedizin</u>. Münster, Westfälische Wilhelms-Universität. **Dr. rer. medi.**

Jansen, A., M. Deppe, et al. (2006). "Interhemispheric dissociation of language regions in a healthy subject." <u>Arch Neurol</u> **63**(9): 1344-6.

Jansen, A., C. Sehlmeyer, et al. (2009). "Assessment of verbal memory by fMRI: lateralization and functional neuroanatomy." <u>Clin Neurol Neurosurg</u> **111**(1): 57-62.

Jokeit, H., M. Okujava, et al. (2001). "Memory fMRI lateralizes temporal lobe epilepsy." <u>Neurology</u> **57**(10): 1786-93.

Kloppel, S. and C. Buchel (2005). "Alternatives to the Wada test: a critical view of functional magnetic resonance imaging in preoperative use." <u>Curr Opin Neurol</u> **18**(4): 418-23.

Knecht, S., A. Jansen, et al. (2003). "How atypical is atypical language dominance?" <u>Neuroimage</u> **18**(4): 917-27.

Krach, S. (2006). Hemisphärenspezifische Aktivierung bei der mentalen Reim- und Wortgerierung mittels funktioneller Magnetresonanztomographie (fMRT) und funktioneller transkranieller Dopplersonographie (fTCD) im Vergleich. <u>Fakultät für Pschologie und Sportwissenschaften</u>. Bielefeld, Universität Bielefeld. **Dr.phil.:** 184.

Machielsen, W. C., S. A. Rombouts, et al. (2000). "FMRI of visual encoding: reproducibility of activation." <u>Hum Brain Mapp</u> **9**(3): 156-64.

Minear, M. and D. C. Park (2004). "A lifespan database of adult facial stimuli." <u>Behav Res Methods Instrum Comput</u> **36**(4): 630-3.

Narayan, V. M., D. Y. Kimberg, et al. (2005). "Experimental design for functional MRI of scene memory encoding." <u>Epilepsy Behav</u> **6**(2): 242-9.

Nolte, J. (2009). <u>The human brain: an introduction to its functional anatomy</u>, Mosby/Elsevier.

Oldfield, R. C. (1971). "The assessment and analysis of handedness: the Edinburgh inventory." <u>Neuropsychologia</u> **9**(1): 97-113.

Powell, H. W., M. J. Koepp, et al. (2004). "The application of functional MRI of memory in temporal lobe epilepsy: a clinical review." <u>Epilepsia</u> **45**(7): 855-63.

Powell, H. W., M. J. Koepp, et al. (2005). "Material-specific lateralization of memory encoding in the medial temporal lobe: blocked versus event-related design." <u>Neuroimage</u> **27**(1): 231-9.

Putcha, D., K. O'Keefe, et al. (2011). "Reliability of functional magnetic resonance imaging associative encoding memory paradigms in non-demented elderly adults." Hum Brain Mapp **32**(12): 2027-44.

Rosazza, C., L. Minati, et al. (2009). "Engagement of the medial temporal lobe in verbal and nonverbal memory: assessment with functional MR imaging in healthy subjects." AJNR Am J Neuroradiol **30**(6): 1134-41.

Ruprecht, C., Gruppe H., Gebhardt H., Bauer E., Sammer G. (2009). DataWeasel Giessen, Cognitive Neurosience - Center for Psychiatry Giessen, CNS@ZPG, Justus Liebig Universität Giessen**:** Logfile analysis search, filter, calculate, and batch mode with graphical user interface.

Scoville, W. B. and B. Milner (1957). "Loss of recent memory after bilateral hippocampal lesions." J Neurol Neurosurg Psychiatry **20**(1): 11-21.

Sehlmeyer, C. (2006). Entwicklung eines Paradigmas zur Bestimmung von Gedaechtnislateralisation – Eine fMRT-Studie. Muenster. **Dipl. Psych:** 78.

Shrout, P. E. and J. L. Fleiss (1979). "Intraclass correlations: uses in assessing rater reliability." Psychol Bull **86**(2): 420-8.

Specht, K., K. Willmes, et al. (2003). "Assessment of reliability in functional imaging studies." J Magn Reson Imaging **17**(4): 463-71.

SPM. (2009). "SPM 8." from http://www.fil.ion.ucl.ac.uk/spm/.

Squire, L. R. (1992). "Memory and the hippocampus: a synthesis from findings with rats, monkeys, and humans." Psychol Rev **99**(2): 195-231.

Strandberg, M., C. Elfgren, et al. (2011). "fMRI memory assessment in healthy subjects: a new approach to view lateralization data at an individual level." Brain Imaging Behav **5**(1): 1-11.

Trepel, M. (2008). Neuroanatomie: Struktur und Funktion ; [Online-Zugang + interaktive Extras], Urban & Fischer bei Elsev.

Wagner, K., L. Frings, et al. (2005). "The reliability of fMRI activations in the medial temporal lobes in a verbal episodic memory task." Neuroimage **28**(1): 122-31.

Wigan, A. L. (1844). A New View of Insanity: The Duality of the Mind Proved by the Structure, Functions and Diseases of the Brain and by the Phenomena of Mental Derangement and Shown to be Essential to Moral Responsibility, Longman.

Worsley, K. J., S. Marrett, et al. (1996). "A unified statistical approach for determining significant signals in images of cerebral activation." Hum Brain Mapp **4**(1): 58-73.

Yang, J., P. Pan, et al. (2012). "Voxelwise meta-analysis of gray matter anomalies in Alzheimer's disease and mild cognitive impairment using anatomic likelihood estimation." J Neurol Sci **316**(1-2): 21-9.

Meine akademischen Lehrer waren:

Damen/Herren in Marburg:	Damen/Herren in Lübeck:	Damen/Herren in Gießen:
Basler	Borck	Bödecker
Baum	Gillessen-Kaesbach	Derrmeyer
Brehm	Krüger	Diemer
Cetin	Seyfarth	Eikmann
Daut		Füssle
Eilers		Gallhofer
Feuser		Gieler
Glorius		Goebeler
Grundmann		Grebe
Klose		Hörbelt
Koolmann		Kaps
Lill		Karg
Löffler		Kemkes-Matthes
Mandrek		Klußmann
Mueller		Kreuder
Müller		Kruse
Müller-Brüsselbach		Lange
Röhm		Lorenz
Seitz		Mayer
Westermann		Rau
		Repp
		Reuter
		Rickert
		Schäffer
		Schneider
		Tinneberg
		Weigand
		Willems

Danksagung

Mein größter Dank gilt Herrn Univ.-Prof. Dr. A. Jansen für die intensive Betreuung, die viele Hilfe bei dem Projekt, die großartige Unterstützung und die lehrreiche und angenehme gemeinsame Zeit.

Ein besonderer Dank geht an Dr. Jens Sommer ohne den die technische Realisierung der Versuche nicht mögliche gewesen wäre.

Ein weiterer Dank an Johannes Bedenbender für den Kontakt zur Arbeitsgruppe, seine Unterstützung bei der Programmierung der Paradigmen und der Auswertung der Logfiles.

Mein Dank gilt auch der medizinisch-technischen Angestellten Mechthild Wallnig für die Hilfe bei der Datenerhebung.

Ich möchte mich auch bei Cindy Parsons für die Rechtschreibkorrektur der Arbeit bedanken.

Abschließend bedanke ich mich besonders meiner Frau Rebekka Brandt für ihre unendlich liebevolle Unterstützung und bei meinen Eltern Burkhard und Christa Brandt, die mich immer unterstützt haben und Vertrauen in meine Arbeit hatten. Bei meinen Geschwistern Naemi Jonas und Stephan Brandt, meinen Cousins Philipp und Claudius, meiner Cousine Rahel, meiner Tante Gertrud und meinem Onkel Jan Deters, die mich vor allem in der Frühphase unterstützt haben. Außerdem bedanke ich mich bei allen Freunden und Bekannten die mich während der Zeit unterstützt haben.